

Spring 2024

## Feasibility of Pile Driving Analyzer for Pile On Rock

Tanvir Ahmed

Follow this and additional works at: <https://digitalcommons.georgiasouthern.edu/etd>



Part of the [Geotechnical Engineering Commons](#)

---

### **Recommended Citation**

Ahmed, Tanvir, "Feasibility of Pile Driving Analyzer for Pile On Rock" (2024). *Electronic Theses and Dissertations*. 2779.

<https://digitalcommons.georgiasouthern.edu/etd/2779>

This thesis (open access) is brought to you for free and open access by the Jack N. Averitt College of Graduate Studies at Georgia Southern Commons. It has been accepted for inclusion in Electronic Theses and Dissertations by an authorized administrator of Georgia Southern Commons. For more information, please contact [digitalcommons@georgiasouthern.edu](mailto:digitalcommons@georgiasouthern.edu).

# FEASIBILITY OF PILE DRIVING ANALYZER FOR PILE ON ROCK

by

TANVIR AHMED

(Under the Direction of Soonkie Nam)

## ABSTRACT

The purpose of the field verification of piles is to check whether piles can withstand design load. Two commonly used methods are high strain dynamic piles and static load testing. Static load testing is very time-consuming, requires heavy deadloads and much space, and doesn't have stress monitoring advantages in piles. High strain dynamic has been employed as an alternative in this regard. Pile dynamic analyzer (PDA) is a device which is used during dynamic testing to analyze the measurements from the test. PDA calculates the geotechnical or structural resistance by using wave mechanics algorithm installed in it. Total driving resistance (or geotechnical resistance) consists of dynamic and static resistance. In PDA, the pile capacity is considered as static resistance which is calculated using Case formula. In this formula, a Case damping factor which represents ground condition needs to be selected carefully since it affects the estimation of maximum pile capacity (RMX). It was found that 0.9 of Case damping factor was used in the reviewed projects with PDA. This is believed to be irrelevant to the ground conditions. Therefore, the estimated ultimate pile capacity (RMX) could be questionable. However, this issue is not supposed to be critical as the final estimation of the pile capacity is estimated by the result of CAPWAP analysis. It has not been confirmed whether the Case damping factor estimated by CAPWAP represents the ground conditions well, especially for rock. Hence, the Case damping factor from CAPWAP still needs to be verified, preferably by static load test. However, it is expected to be very uneconomical for rock, thus alternative methods are recommended for

investigation. The CAPWAP damping factors grouped by Banks and Cobb Counties show a good trend against blows per inch in each group. However, it still needs to be interpreted carefully as the other factors affect the penetration of a pile.

INDEX WORDS: Wave Mechanics, Pile driving analyzer, Hard rock, Weak rock, Static load testing, Dynamic testing.

FEASIBILITY OF PILE DRIVING ANALYZER FOR PILE SEATED ON ROCK

by

TANVIR AHMED

B.S., Shahjalal University of science & technology, Bangladesh, 2021

A Thesis Submitted to the Graduate Faculty of Georgia Southern University

in Partial Fulfillment of the Requirements for the Degree

MASTER OF SCIENCE

ALLEN E. PAULSON COLLEGE OF ENGINEERING AND COMPUTING

© 2024

TANVIR AHMED

All Rights Reserved

FEASIBILITY OF PILE DRIVING ANALYZER FOR PILE SEATED ON ROCK

by

TANVIR AHMED

Major Professor:  
Committee:

Soonkie Nam  
Gustavo Maldonado  
Xiaoming Yang

Electronic Version Approved:  
May 2024

## DEDICATION

I would like to dedicate this thesis to my family and to my friends. Their constant support, prayers, and encouragement have pushed me to go above and beyond in everything I do.

## ACKNOWLEDGMENTS

I am grateful to Georgia Department of Transportation for their support for this research. I appreciate the College of Graduate Studies for financial support to my study. I am very grateful to Dr. Soonkie Nam for his relentless support and excellent supervision in this research. I am thankful to the committee members Dr. Gustavo Maldonado and Dr. Xiaoming Yang for their support in this research. I express my gratitude to Dr. Marcel Maghiar, Dr. Gustavo Maldonado and Dr. Nam for providing me with the opportunity to work with them in their GDOT project. I appreciate the support of all course instructor I worked with. I also acknowledge undergraduate student Ana Lanza and Anu Pradeep since I worked with them in several research and competition and gathered valuable experiences. for her contribution to this project.

## Table of Contents

	Page
ACKNOWLEDGMENTS .....	3
CHAPTER 1 .....	9
INTRODUCTION.....	9
1.1 Purpose of the Study .....	9
CHAPTER 2 .....	12
LITERATURE REVIEW.....	12
CHAPTER 3 .....	15
THEORY BEHIND PILE DRIVING ANALYZER.....	15
3.1 Pile Driving Formula.....	15
3.1.1 Concept of Energy Conservation .....	15
3.2 Smith’s Approach .....	21
3.3 Geotechnical Resistance .....	23
3.3.1 Geotechnical Static Resistance .....	24
3.3.2 Geotechnical Dynamic Resistance.....	25
3.4 Pile Driving Analyzer (PDA) .....	26
3.4.1 Generation of Force and Velocity Curve of Pile Top.....	26
3.4.2 Bearing Capacity using PDA.....	35
CHAPTER 4 .....	37
VERIFICATION OF THE PDA ANALYSIS USING FIELD TEST DATA .....	37
4.1 Introduction .....	37
4.2 Banks County, Georgia.....	37
4.3 Cobb County, Georgia.....	40
4.4 Wake County, North Carolina.....	42
CHAPTER 5 .....	45
RESULTS.....	45
5.1 Analysis of PDA test result .....	45

CHAPTER 6 ..... 49

    CONCLUSIONS And RECOMMENDATIONS ..... 49

REFERENCES ..... 51

APPENDIX A..... 53

## LIST OF TABLES

Table 1: Recommended Damping factor (Ng et al. 2011).....	13
Table 2: Pile design parameters in Banks County .....	38
Table 3: Uniaxial compressive strength of the rock samples at bent 3.....	39
Table 4: PDA test results in Banks County .....	39
Table 5: Pile design parameters in Cobb County.....	40
Table 6: PDA test results in Cobb County .....	42
Table 7: PDA test results in Wake County .....	42
Table 8: Summary of PDA test input parameters .....	43
Table 9: Calculated $Q_{total}$ from two different approaches. ....	46
Table 10: RMX vs Case Damping Factor.....	46
Table 11: RMX & Case damping factor values from PDA and CAPWAP.....	47

## LIST OF FIGURES

Figure 1: Resistance-displacement of piles for each hammer blow. ....	16
Figure 2: Hammer drop height vs pile set.....	17
Figure 3: Pile element subjected to compressive wave travelling in the z direction .....	20
Figure 4: Smith model (Modified from Rausche et al. (2004)) .....	22
Figure 5: Pile-ground interaction .....	23
Figure 6: Development of static resistance during driving.....	24
Figure 7: Geotechnical dynamic resistance .....	25
Figure 8: Typical pile test setup.....	26
Figure 9: Piles at rest before subject to dynamic impact .....	27
Figure 10: At the moment of impact.....	27
Figure 11: Effect of downward compressive wave over $z$ .....	29
Figure 12: Pile top force and velocity at $t_0$ .....	30
Figure 13: Effect of downward compressive wave over $L_n$ .....	30
Figure 14: Piles top force and velocity until $tn$ .....	31
Figure 15: Effect of downward compressive wave over $L$ .....	31
Figure 16: Pile top force and velocity until $t_0 + Lc$ .....	32
Figure 17: Effect of upward compressive wave over $L$ .....	34
Figure 18: Pile top force and velocity for full time record .....	34
Figure 19: Pile top force and velocity for full time record .....	35
Figure 20: Pile top force and velocity.....	36
Figure 21: Banks County project layout (GDOT Office of Materials and Testing 2021).....	38

Figure 22: Cobb County project layout of bridge number 4 (GDOT Office of Materials and Testing 2021) .....	41
Figure 23: PDA field test at Banks County, Georgia, USA.....	43
Figure 24: CAPWAP recommended Damping factor vs blows per inch at Banks and Cobb County.....	48
Figure 25: Pile top force and velocity (Bent 1-Blow 236) .....	53
Figure 26: Pile top force and velocity (Bent 3-Blow 4) .....	53
Figure 27: Pile top force and velocity (Bent 3-Blow 5) .....	54
Figure 28: Pile top force and velocity (Bent 3-Blow 6) .....	54
Figure 29: Pile top force and velocity (Bent 4-Blow 95) .....	55
Figure 30: Pile top force and velocity (Bent 4-Blow 131) .....	55
Figure 31: Pile top force and velocity (Bent 4-Blow 145) .....	56
Figure 32: Pile top force and velocity (Bent 5-Blow 6) .....	56
Figure 33: Pile top force and velocity (Bent 14-Blow 27) .....	57
Figure 34: Pile top force and velocity (Bent 1-Blow 5) .....	57

## CHAPTER 1

### INTRODUCTION

#### 1.1 Purpose of the Study

The purpose of foundation of a structure is to transfer vertical and lateral loads from superstructures to soil or rock. The choice of foundation (shallow or deep foundation) type is generally based on considerations of structural requirements, subsurface conditions, site characteristics and economics. Deep foundations (also referred as Pile Foundations) are utilized when shallow type foundations do not provide adequate support.

Pile foundation is the oldest and widely used method owing to their higher bearing capacity and ability to overcome problems arise from weak soil formation (Liu et al. 2020). The ultimate capacity of piles is the amount of highest load that can be carried by a pile without failure or undergoing excessive settlement. Several different theoretical procedures have been proposed for determination of ultimate capacity of bored or driven piles. However, even if very careful job is done with piles type selection, design, and construction, without field test on the constructed pile, excessive uncertainty remains. Static and dynamic load tests are two mentionable field verification methods that are used to reduce these uncertainties.

Static load tests measure the response of a pile under an applied load and are the most accurate method for determining piles capacities. They can determine the ultimate failure load of a foundation pile and determine its capacity to support the load without excessive or continuous displacement (California and Transportation 2008). However, this method has some disadvantages including being time-consuming, less safe, requiring excessive dead loads and spaces, obstructing the movement of traffic, and having difficulty separating toe resistance from total resistance. In addition, monitoring of stresses experienced by pile is not available in this test (Salgado 2008).

However, dynamic test has the capability to overcome some these drawbacks associated with static load test (Rausche et al. 2006).

Dynamic tests work on the basis of dynamic formula or driving formula such as Sanders' formula of 1851, Engineering News formula, Morrison formula of 1868, Dutch formula of 1812, Weisbach's formula of 1850, Janbu formula 1953, Danish formula 1957, Hiley's formula of 1925, Cornfield formula 1961 (purely empirical) and Wave Equation. All of these formulae except wave equation and purely empirical equation work on the assumption that a force is generated instantly throughout the pile on impact, which is incorrect. More realistically, pile behaves like an elastic rod, and pile driving depends on the transmission of compressive wave travel down the piles on which wave equation fits in (Whitaker 2013).

By integrating soil resistance and the wave equation applied to each element of pile, Smith (1960) introduced a finite element approach. To perform the calculation, a pile is divided into a number of lengths and masses. Each element is connected to the adjacent element by springs. The hammer and cushion are represented by a weight and spring at the head. Soil resistances are applied to the weights to represent the shaft friction and the base resistance.

Wave Equation Analysis Program (WEAP) and Pile Driving Analyzer (PDA) are two mentionable dynamic tests which have been developed on the concept of the above approach. WEAP is done before driving to verify pile capacity and drivability. Comparatively, PDA is more widely accepted since it is performed during pile driving, providing the real-time results in the field (So and Ng 2011).

PDA requires measurement of strains and accelerations of pile elements near the pile head as hammer strikes the piles head which (strains and accelerations) are converted to force and velocity respectively. From pile top force and velocity data, PDA computes mobilized

geotechnical resistance using Case formula. In this formula, geotechnical resistance is assumed to be located entirely at the pile base. Geotechnical resistance consists of dynamic and static resistance. In PDA, the pile capacity is considered as static resistance. However, to calculate the pile capacity (static resistance), first dynamic resistance is calculated. The subtraction of the calculated dynamic resistance from the total resistance yields static resistance. The dynamic resistance depends on case damping, pile impedance and pile base velocity. In dynamic resistance, ground condition is addressed through case damping factor. Use of the same or inappropriate damping factor may lead to unreasonable estimation of dynamic resistance. Therefore, static resistance will not represent the actual pile capacity if estimated dynamic resistance is questionable. Soil, silt and clay have well established damping factor (Ng et al. 2011). For rock, there is no recommended damping factor available. Hence, this study sheds light on the performance of the PDA test on rock in terms of damping factor.

## CHAPTER 2

### LITERATURE REVIEW

Several researchers worked on the applicability of PDA on rock. Some researchers focused on quake and damping values of rock when PDA is used for pile capacity verification. On the other hand, some researchers compared the PDA results with static load test and structural limit load of pile.

Ng and Sullivan (2017) used static analysis methods to estimate the geotechnical resistances of pile driven on rock. All driven piles ended up on rock layer. Pile driving analyzer and wave equation analysis program were utilized to verify the performances of pile during construction. Structural capacity was used as performance criteria to evaluate static analysis method, wave equation analysis program and PDA. At the end of driving, 49 piles (72%) were deemed unacceptable when PDA was used since PDA calculated geotechnical resistance did not satisfy the LRFD strength limit state. The authors recognized in the research that the PDA as dynamic test is not a proof load test since it does not provide reasonable estimation of geotechnical resistance.

So and Ng (2011) mentioned in his study that dynamic testing changes the ground leading to densification, loosening, liquefaction and set-up. In rock, the impact force is not enough to fully activate the rock below the pile base when rock shows limited movement and yielding. During pile driving, pile movement and base velocity are affected due to installation method, load-transfer mechanism. Hence, Case damping is also affected due to variable pile movement and pile base velocity. Since Case damping contributes to the dynamic resistance of PDA, dynamic resistance also changes when Case damping is affected. Eventually, the inaccurate estimation of dynamic resistance causes unreasonable calculation of ultimate pile resistance.

In the research of Abeysinghe (2003), determination of a range of damping values for rock socketed piles was focused on. Quake represents maximum elastic deformation of ground. Maximum elastic deformation of ground activates full static resistance. If piles penetration under hammer blow is high, the quake value is also high. Large pile base quake values have been observed in soil. However, it is very hard to give a considerable amount of deformation to rock. The researcher found that case damping varies from 0.15 to 0.35 for rock socket piles.

According to Goble, Likins, and Rausche (1975), the dynamic resistance is important only at the time pile driving. The dynamic resistance has no practical value. Since, total resistance in PDA test comes from static and dynamic resistance, the pile capacity is considered as static resistance. However, to calculate the pile capacity static resistance, dynamic resistance must first be calculated. The subtraction of the calculated dynamic resistance from the total resistance results in static resistance. Dynamic resistance depends on case damping ( $J_c$ ), pile impedance ( $Z$ ) and pile base velocity ( $V_b$ ). Case damping represents ground condition at pile base. Goble, Likins, and Rausche (1975) recommended some damping factor for sand, silt and clay. These recommended values were updated later which can be seen in Table 1.

Table 1: Recommended Damping factor (Ng et al. 2011)

<b>Ground Type</b>	<b>Original Case Damping factor</b>	<b>Updated Case Damping factor</b>
Clean Sand	0.05 to 0.20	0.10 to 0.15
Silty Sand, Sand Silt	0.15 to 0.30	0.15 to 0.25
Silt	0.20 to 0.45	0.25 to 0.40
Silty Clay, Clayey Silt	0.40 to 0.70	0.40 to 0.70
Clay	0.60 to 1.10	0.70 or higher

In PDA, the static component of the geotechnical resistance can be taken as the limit load on pile if the hammer blow is sufficiently powerful to mobilize it fully. As the pile is driven to refusal, penetration induced by the hammer blow may not be sufficient to mobilize the limit load.

In such cases, a smaller static capacity which is considered to be an estimate of the ultimate load is mobilized (Salgado 2008).

## CHAPTER 3

## THEORY BEHIND PILE DRIVING ANALYZER

## 3.1 Pile Driving Formula

Pile driving Formulae (also known as dynamic formulae) are based on the notion “The effort needs to drive a stake into the ground depends on the Resistance of the ground”. They owe their existence to the assumption that total ground resistance to driving is equivalent to ultimate bearing capacity of the pile under static loading. The following symbols are used for all formulae (Whitaker 2013).

$W$  = Hammer weight

$P$  = Pile weight

$H$  = Hammer fall height

$R$  = Ground driving resistance

$s$  = Set, i.e. net distance pile is driven after unloading.

$A$  = Pile cross-sectional area

$L$  = Pile length

$E$  = Young’s Modulus of pile material.

## 3.1.1 Concept of Energy Conservation

Upon impact, Equation 1 assumes hammer provides its entire energy on pile head. This generates a resistance  $R$  to the motion of pile which remains constant as the pile moves a distance  $s$ . The available hammer energy is  $WH$ , and the work done in overcoming the resistance is  $Rs$ . Thus, the relation between hammer energy and ground resistance can be seen in Equation 1 which represents Sanders Formula (1851). (Whitaker 2013)

$$WH = Rs$$

Equation 2 follows Sanders Formula (Equation 1) in addition to assumption “for each hammer blow, the ground resistance increases to  $R$  in an elastic manner as the soil is displaced, remains constant for further displacement and then falls to zero in an elastic manner as pile rebounds.” The Equation 2 can be demonstrated with Figure 1 where  $OD = s + c$  is the total displacement.  $c$  represents elastic displacement of pile head. Total work done against the resistance in reaching  $OD$  is area  $OABD$ . Since  $c$  is amount pile rebounds, the work needs to displace  $c$  amount is area  $BDC$ . So, the net soil displacement would be  $OB = s$  associated with area  $OABC$ .

$$\text{Total work} = OABD = OABC + BDC$$

$$WH = Rs + \frac{1}{2}Rc \quad 2$$

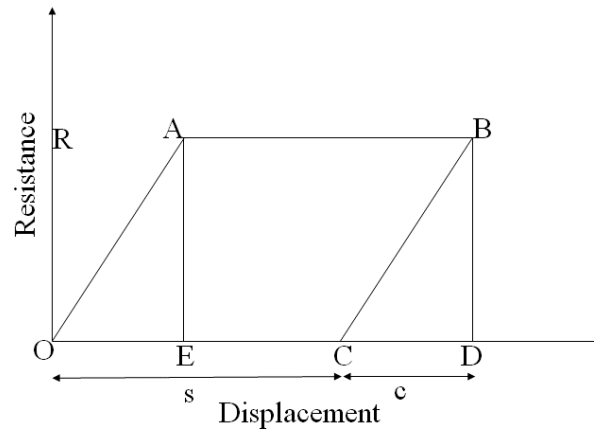


Figure 1: Resistance-displacement of piles for each hammer blow.

Wellington et al. (1893) developed a formula which is similar to Equation 2. His formula was termed Engineering News Formula. In this formula, empirical values are given to  $\frac{c}{2}$ . For examples, if drop hammer is used then numerical value of  $\frac{c}{2}$  would be 1 (Equation 3). Again, if single acting steam hammers is used then the  $\frac{c}{2}$  would be equal to 0.1 (Equation 4) (Whitaker

2013). According to Noorzad, Karimpour-fard, and Mohammadi (2008),  $c$  is a function of hammer type.

$$WH = R(s + 1) \quad 3$$

$$WH = R(s + 0.1) \quad 4$$

The assumptions of Equation 5 align with those of Equation 2. Referring to Figure 1, hammer energy should be more than highest elastic ground resistance to drive a pile. The work done against the highest elastic ground resistance is OAE. If the required height of hammer fall for OAE is  $H_0$ , then equivalent hammer energy is  $WH_0$ . Figure 1 indicates the following relation.

$$\text{OAE} = \text{BDC} = \frac{1}{2}Rc$$

$$WH = Rs + WH_0 \quad 5$$

$H_0$  can be found practically by plotting different hammer drop heights and corresponding sets. The intercept of the linear regression line indicates  $H_0$  (Figure 2)

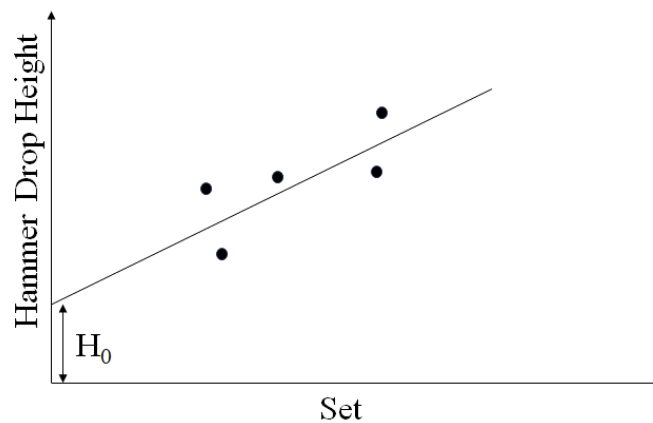


Figure 2: Hammer drop height vs pile set.

According to Morrison (1868),  $s_1$  and  $s_2$  are two piles set for drop height  $H_1$  and  $H_2$  respectively (Whitaker 2013). Therefore, solution of the resistance can be found from Eqn. 6 and

$$WH_1 = Rs_1 + \frac{1}{2}Rc \quad 6$$

$$WH_2 = Rs_2 + \frac{1}{2}Rc \quad 7$$

$$W(H_1 - H_2) = R(s_1 - s_1) \quad 8$$

Equation 9 considers  $U$  as energy supplied by hammer impact not useful in driving a pile. Applying Newton's law on impact between hammer and pile, the energy equation can be represented by Equation 10 which is Dutch (1861) formula (Noorzad, Karimpour-fard, and Mohammadi 2008).

$$WH = Rs + U \quad 9$$

$$Rs = \frac{W^2H}{W + P} \quad 10$$

Equation 11 or Weisbach's formula (1850) considers the energy equation  $WH = Rs + U$  (Equation 9) where  $U$  is defined as elastic compression of pile as if it were a strut under a static load  $R$  (Whitaker 2013). The elastic compression of pile is  $RL/AE$  and the elastic energy is  $R^2L/2AE$ . So, the energy equation can be rewritten as

$$WH = Rs + \frac{R^2L}{2AE} \quad 11$$

Considering friction or other losses in hammer system resulting  $KWH$  as available energy at impact, Janbu et al. (1953) proposed following energy equation.

$$\frac{KWH}{(1.5 + 0.3\frac{P}{W})} = Rs + \frac{R^2L}{2AE} \quad 12$$

Where  $K$  is a constant less than 1 (Whitaker 2013). Danish (1957) formula takes into consideration of friction loss in the hammer system along with pile elastic compression

(Abeyasinghe 2003). If all available hammer energy is used in compressing the pile, the energy equation would be

$$KWH = R_s + \frac{R}{2}(2KWHL/AE)^{0.5} \quad 13$$

Hiley's formula (1925) assumes the following energy losses.

- In the hammer system
- Due to impact
- Due to piles elastic compression  $c_p$
- Due to elastic compression  $c_c$  of dolly, helmet and packing
- Due to ground elastic compression  $c_q$

Considering these factors Hiley et al. (1925) proposed the following formula.

$$R = WH\eta/(s + c/2) \quad 14$$

Where  $\eta = K(W + e^2P)/(W + P)$  and  $c = c_c + c_p + c_q$

Cornfield (1964) proposed an empirical formula which is only applied to concrete pile having 20-80 ft length, hammer drop height of 3-5ft and, set not exceeding 0.33 inch per blow (Whitaker 2013). The expression is shown below where L is the pile length.

$$R = 0.08 * W(2 + H)(140 - L)(1 - s) \quad 15$$

Wave mechanics assume pile driving a phenomenon of compression waves travelling down the piles. It also considers pile to behave like an elastic rod. Let's consider a pile (slender) element surrounded by less stiff materials (Figure 3). When a pile is struck by a hammer, a compressive wave travels up and down the pile. Considering a finite element  $dz$  in length in the pile which experiences  $Q$  compressive force in the downward direction and  $Q + dQ$  compressive wave in the upward direction.

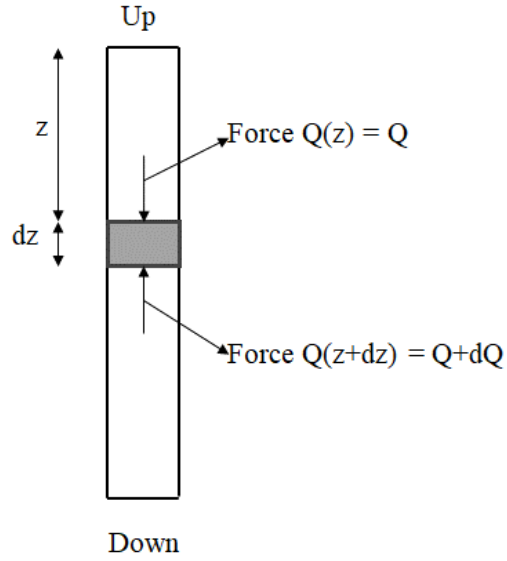


Figure 3: Pile element subjected to compressive wave travelling in the  $z$  direction

Application of Newton's second law  $\sum F = ma$  to this element yields

$$Q - (Q + dQ) = \rho A dz \frac{\partial^2 w}{\partial t^2} \quad 16$$

$$-dQ = \rho A dz \frac{\partial^2 w}{\partial t^2} \quad 17$$

Where  $w$  = axial displacement of pile cross-section,  $\rho$  = pile mass density,  $A$  = pile cross sectional area. If we rewrite Equation 17 with  $dQ = \frac{\partial Q}{\partial z} dz$  it will turn into following equation

$$-\frac{\partial Q}{\partial z} dz = \rho A dz \frac{\partial^2 w}{\partial t^2} \quad 18$$

$$-\frac{\partial Q}{\partial z} = \rho A \frac{\partial^2 w}{\partial t^2} \quad 19$$

From elastic relationship for stress  $\sigma = E\varepsilon$  and strain  $\varepsilon = -\frac{\partial w}{\partial z}$  we can rewrite Equation 19

$$EA \frac{\partial^2 w}{\partial z^2} = \rho A \frac{\partial^2 w}{\partial t^2} \quad 20$$

$$\frac{\partial^2 w}{\partial z^2} = c^2 \frac{\partial^2 w}{\partial t^2} \quad 21$$

Equation 21 is the governing differential equation for a wave of any shape traveling in the  $z$  direction where  $c = \sqrt{\frac{E}{\rho}}$  is wave velocity (Salgado 2008).

### 3.2 Smith's Approach

Figure 4 shows typical Smith's pile-soil model.  $W_2, W_3, \dots, W_b$  denote weight of each pile element. Each element is connected to neighbouring element by pile spring and damping. Also, each element is attached to surrounding soil by soil spring and damping which (spring and damping) represents soil resistance. The spring and damping along with pile skin provide skin resistance, whereas the pile base resistance comes from soil spring and damping below pile base. The hammer and hammer cushion represents weight ( $W_1$ ) and spring respectively. The general equations of force, displacement, and velocity for element  $W_n$  are as follows:

$$D_{nt_i} = D_{nt_{i-1}} + v_{nt_{i-1}} \Delta t \quad 22$$

$$C_n = D_{nt_i} - D_{n+1t_i} \quad 23$$

$$F_n = C_n K_n \quad 24$$

$$a_{nt_{n-1}} = (F_n + W_n - R_n - F_{n-1})/m_n \quad 25$$

$$v_{nt_i} = v_{nt_{i-1}} + a_{nt_{i-1}} \Delta t \quad 26$$

Here,

$D_{nt_i}$  = Displacement of element  $n$  at time  $t_i$

$v_{nt_i}$  = Velocity of element  $n$  at time  $t_i$

$C_n$  = Compression of spring  $n$  at time  $t_i$

$F_n$  = Force exerted (applied) by spring  $n$  at time  $t_i$

$K_n$  = Spring constant of spring  $n$

$W_n =$  Weight of element  $n$

$R_n$  Skin resistance by soil at time  $t_i$

$\Delta t$  Time interval ( $t_i - t_{i-1} = t_{i+1} - t_i = \Delta t$ )

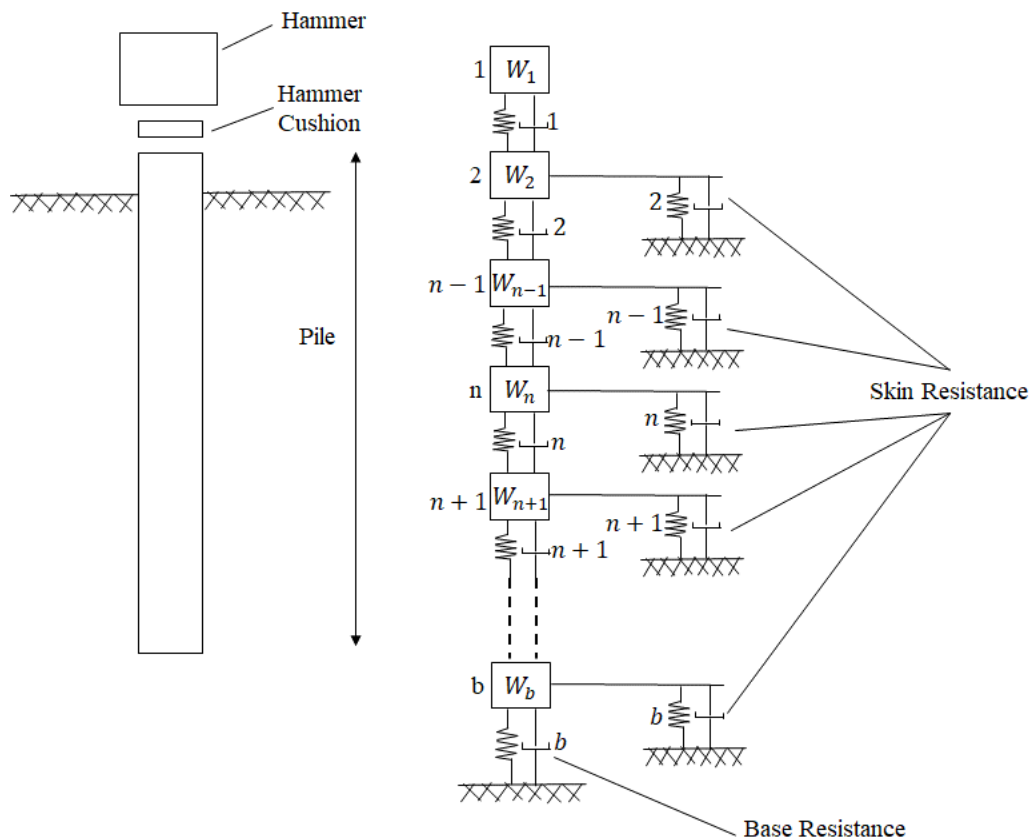


Figure 4: Smith model (Modified from Rausche et al. (2004))

Wave equation analysis is the repetition of relatively straightforward calculations for every pile element. Calculations start at the top of the pile and progress downward. It will take time for the effects of the hammer blow to reach the lower elements of the piles, so calculations initially involve only the top pile elements, and then, more elements until all elements have experienced the effects of the hammer blow.

### 3.3 Geotechnical Resistance

Figure 5 represents typical pile-soil interaction for dynamic test of pile. The pile is connected with the soil in terms of soil stiffness and viscous damping. The pile is assumed to act as an elastic rod whereas visco-elastic plastic behavior is expected to be seen in soil. This soil behavior forms the basis of soil resistance. In the analysis of wave propagation in pile, soil resistance is assumed acting along pile shaft and base. Total soil resistance acting on the pile shaft and base is expressed with the following formula.

$$Q_{total} = Q_{skin} + Q_{base} \quad 27$$

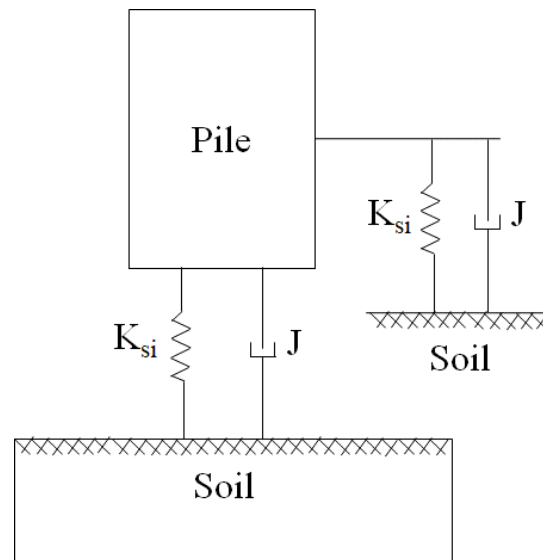


Figure 5: Pile-ground interaction

Each resistance includes static and dynamic resistance corresponding to soil elasticity and viscosity, respectively.

$$Q_{skin} = R_{s(static)} + R_{d(dynamic)} \quad 28$$

$$Q_{base} = R_{s(static)} + R_{d(dynamic)} \quad 29$$

3.3.1 Geotechnical Static Resistance

Figure 6a-Figure 6d represent what happens to soil when the pile, initially at rest, is struck by hammer. Each hammer blow causes some soil deformation  $w_i$ . Initially soil deforms elastically, at shaft and base, up to a limit called quake  $w_{qi}$ . Within this elastic limit  $w_{qi}$  soil resistance increases linearly. At soil's maximum elastic deformation, soil achieves its limit static resistance (Figure 6b). It can be seen in Figure 6c that beyond soil elastic limit  $w_{qi}$ , soil static resistance doesn't go up, and shows plastic behavior with plastic deformation  $w_s$ . It can be stated that lower elastic movement yields low static soil resistance. When complete unloading happens, soil regains its elastic deformation  $w_{qi}$  back but plastic deformation ( $w_s$ ) which is called soil set per hammer blow (Figure 6d).

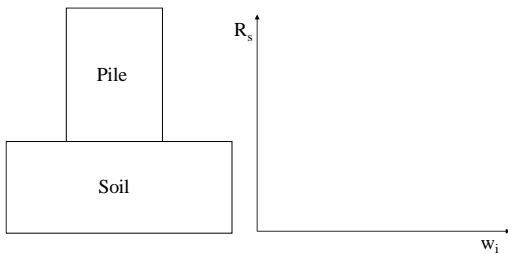


Figure 6a: Before hammer strike.

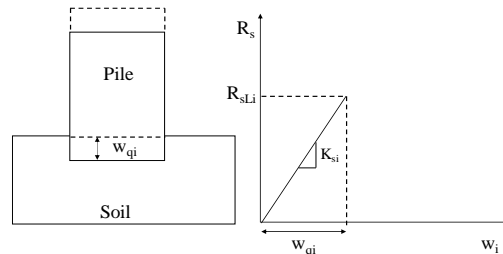


Figure 6b: maximum elastic deformation

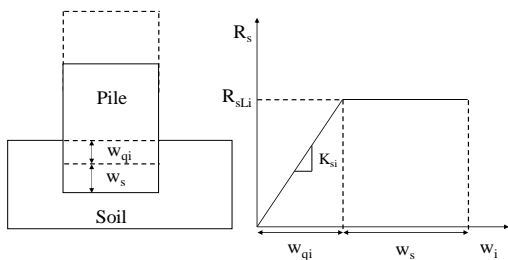


Figure 6c: Plastic deformation

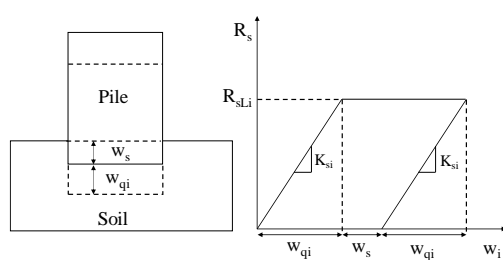


Figure 6d: Deformation after unloading.

Figure 6: Development of static resistance during driving

Equation 30 and 31 shows mathematical form of soil static resistance against pile penetration due to hammering.

$$R_{static} = k_{si}w_i \quad \text{if } w_i < w_{qi} \quad 30$$

$$R_{static} = R_{sLi} \quad \text{if } w_i \geq w_{qi} \quad 31$$

### 3.3.2 Geotechnical Dynamic Resistance

Dynamic soil resistance can be defined as the force exerted by soil for unit velocity of pile tip. It increases linearly with velocity. So, the resistance would be product of a constant velocity. Dynamic soil resistance also depends on damping factor which accounts energy dissipation in the soil, can be modelled as piston-cylinder dashpot (Figure 7). Effect of hammer blow initially act only the top pile elements, then more elements until all elements have experienced the effects of the hammer blow. Dissipation of energy through soil damping reduce the effects for all elements (Salgado 2008). Soil damping can be expressed in two ways: case damping and smith damping. Based on this classification, the following two dynamic resistance formulas have been proposed.

$$R_{dynamic} = J_c Z v_i \quad 32$$

$$R_{dynamic} = J_s R_{sLi} v_i \quad 33$$

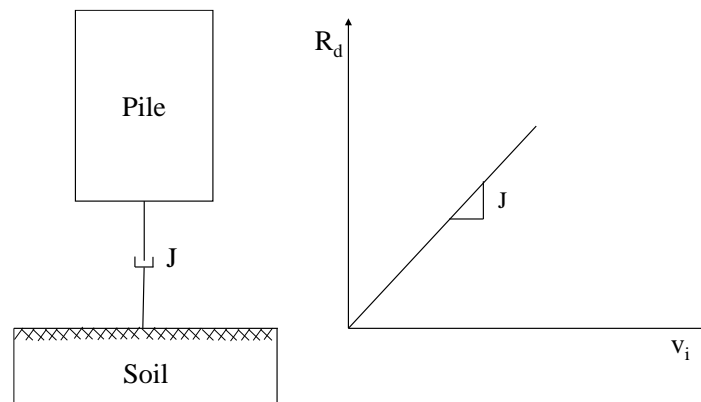


Figure 7: Geotechnical dynamic resistance

In Equation 32,  $J_c$  is a dimensionless parameter and called Case damping factor. Whereas,  $J_s$  has unit and called Smith damping factor in Equation 33.

### 3.4 Pile Driving Analyzer (PDA)

Figure 8 shows a typical PDA test setup. Strain transducer and accelerometer are attached to the top of the pile. A crane is used to drop pile hammer on top of pile to drive the pile to the desired elevation. For each hammer blow, strain and velocity of the pile top are measured by strain transducer and accelerometer, respectively. The recorded strain and velocity of the pile top are sent to a device called Pile Driving Analyzer (PDA). The PDA uses the strain and velocity of the pile top to generate a force and velocity curve of the pile top versus time (from the impact to end of the record for each hammer blow). The section 2.4.1 shows how force and velocity curve of pile top is generated.

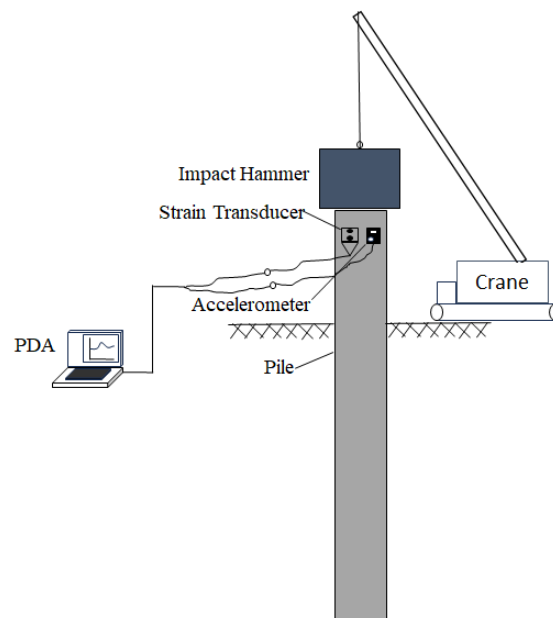


Figure 8: Typical pile test setup

#### 3.4.1 Generation of Force and Velocity Curve of Pile Top

Figure 9-Figure 19 demonstrate what happens when a pile is struck by a hammer. Before hammer strike, it is raised to a predetermined height and dropped on top of pile to make a driving impact (Figure 9).

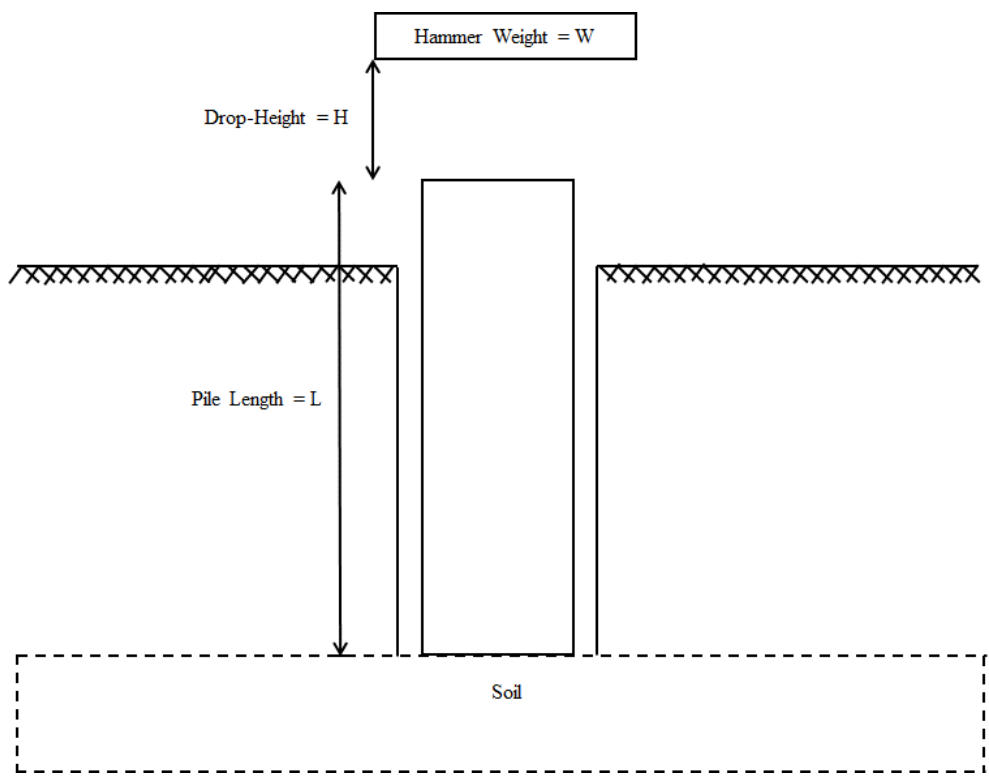


Figure 9: Piles at rest before subject to dynamic impact

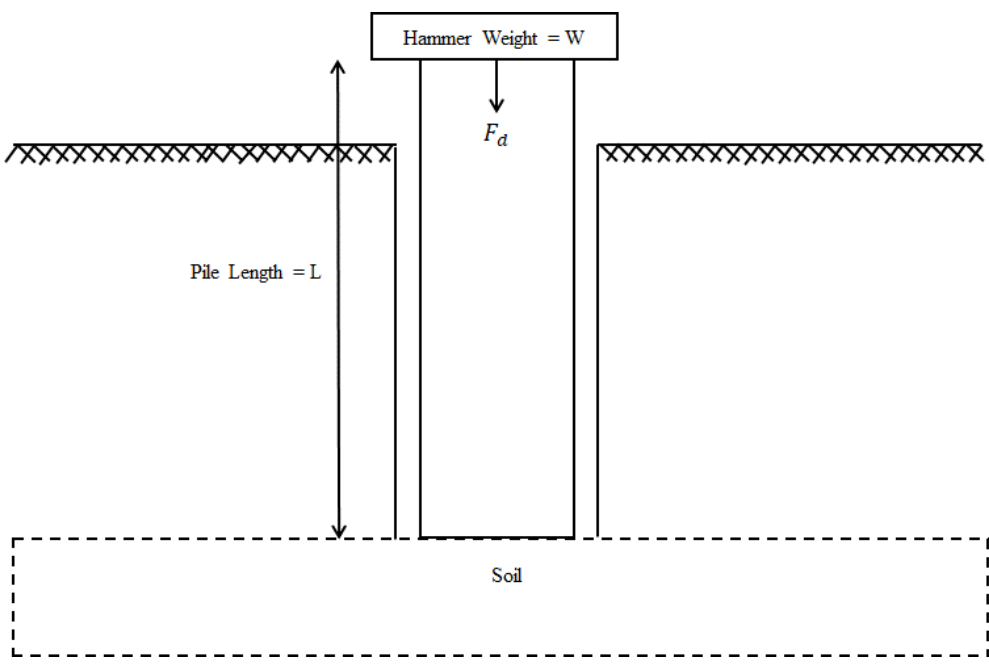


Figure 10: At the moment of impact

Due to impact, it (hammer) transfers its potential energy (WH) into the piles. This impact energy imposes a downward force ( $F_d$ ) at the piles top (Figure 10). This downward force travels down the pile as compressive wave with constant speed “c” and causes downward movement of particles in the pile with velocity ( $v$ ) which is called particle velocity.

Now consider a pile top element with  $z$  length indicated by ash color (Figure 11). After  $t_0$  time, the downward wave passes the top element, hence, the length  $z = ct_0$ . The  $t_0$  is the time where peak of the impact is located. During the same  $t_0$ , particles with speed  $v_1$  in the top element moves  $\Delta z = v_1 t_0$ . These imply that  $z$  amount length of the pile has been strained and  $\Delta z$  amount has been shortened. Now strain over length  $z$  would be following.

$$\varepsilon_z = \frac{\Delta z}{z} = \frac{v_1 t_0}{ct_0} = \frac{v_1}{c} \quad 34$$

From Young modulus formula ( $\sigma = E\varepsilon$  &  $\sigma = F/A$ ), the pile top experiences force  $F_1$  (measured) which can be expressed following way.

$$E = \frac{F_1}{A\varepsilon_z} \quad 35$$

$$E = \frac{F_1}{A \frac{v_1}{c}} \quad 36$$

$$F_1 = \frac{EA}{c} v_1 \quad 37$$

$$F_1 = Zv_1 \quad 38$$

Where  $A$  is pile cross-sectional area and  $Z$  is the pile impedance.

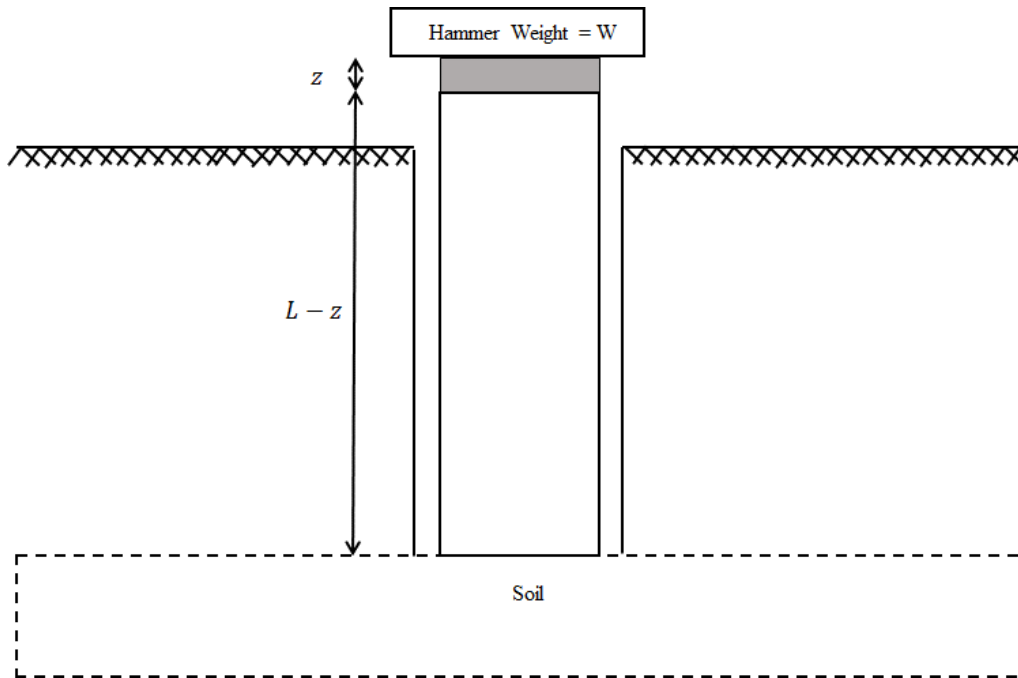


Figure 11: Effect of downward compressive wave over  $z$

The  $t_0$  is the time pile top element experiences highest force and particle velocity due to downward wave (Figure 12). As the wave travels further down the pile, its (wave) effect (measured Force and Velocity) on pile top element varies. After  $t_0 + \frac{L_n}{c}$  time the wave travels a distance  $L_n$  (Figure 13), and at this  $t_0 + \frac{L_n}{c}$  time, the measured force ( $F_2$ ) and velocity ( $v_2$ ) on pile top element (Figure 14) would be different compared to the measured force ( $F_1$ ) and velocity ( $v_1$ ) on pile top element at  $t_0$ . Hence, the relation would be same as Equation 38

$$F_2 = Zv_2$$

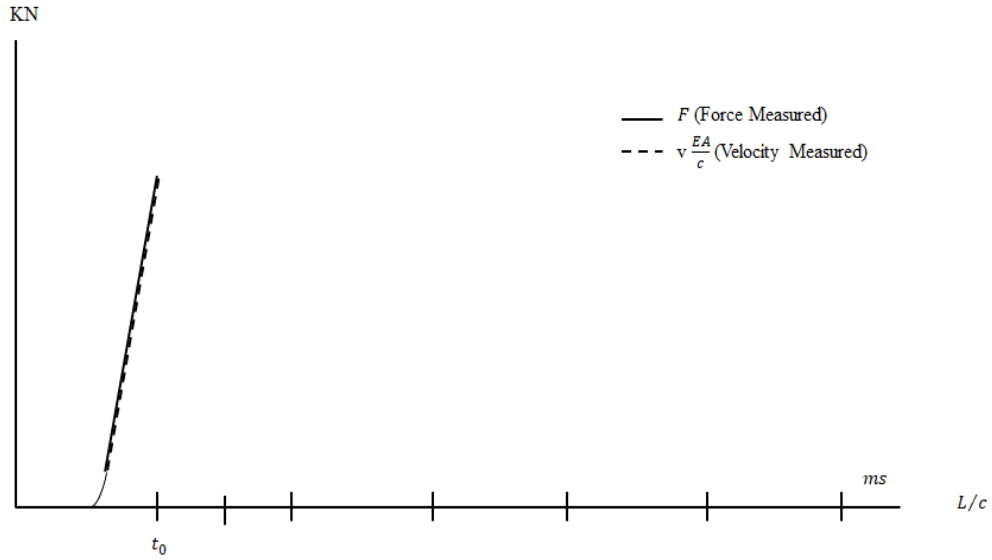


Figure 12: Pile top force and velocity at  $t_0$

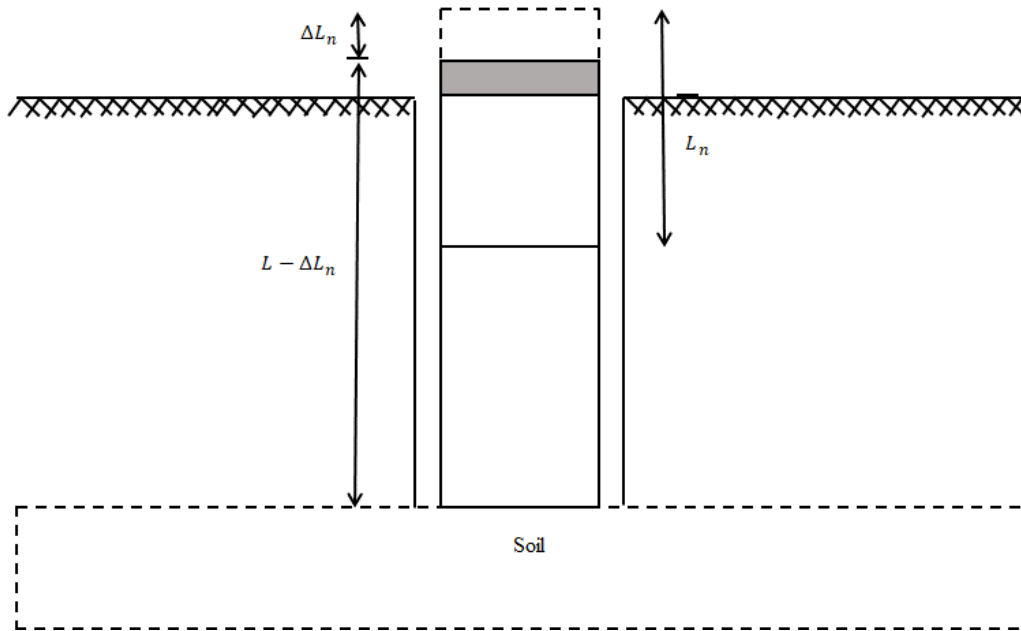


Figure 13: Effect of downward compressive wave over  $L_n$

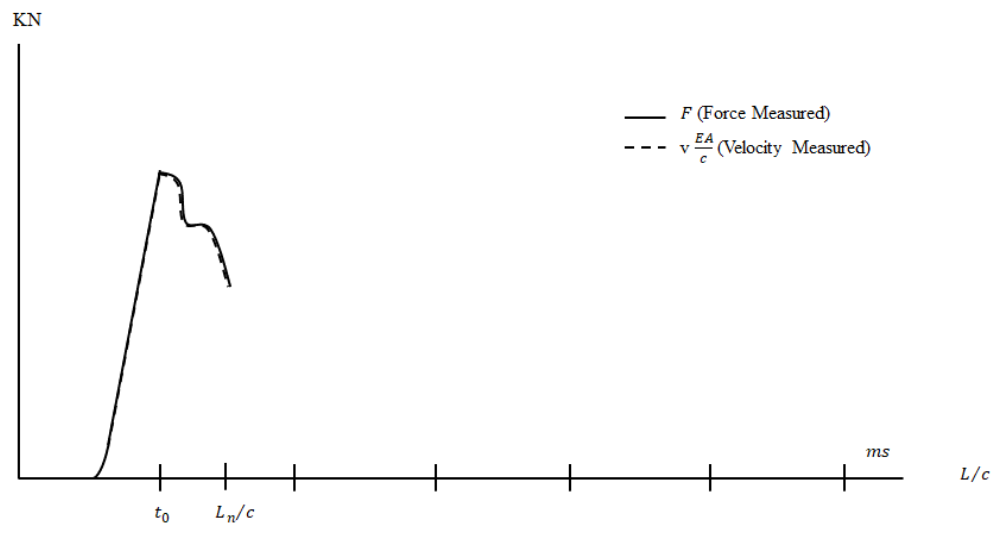


Figure 14: Piles top force and velocity until  $t_n$

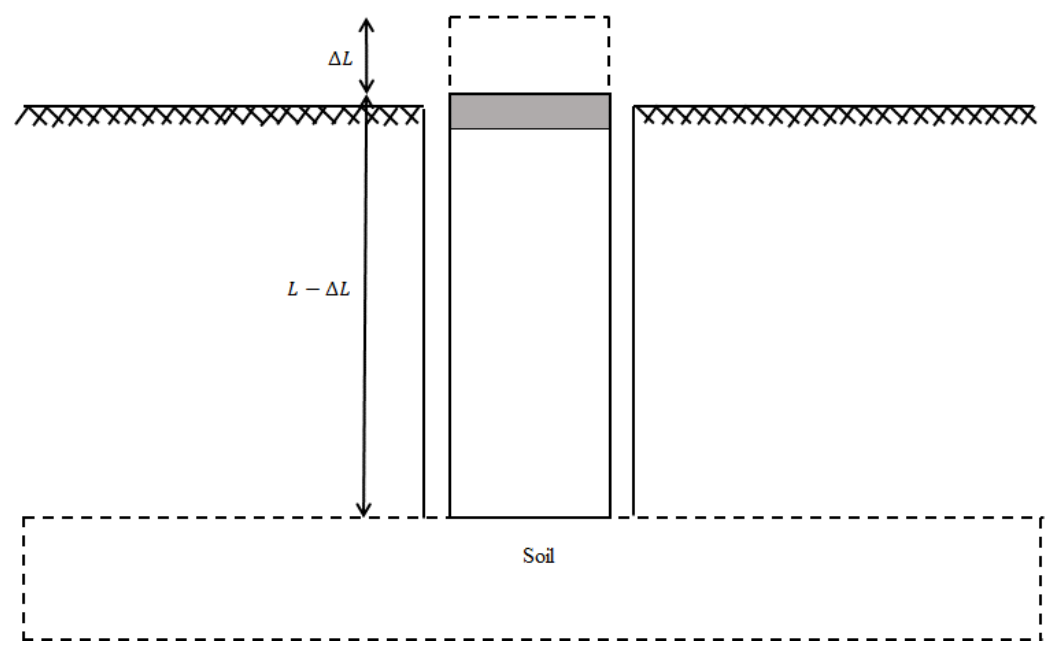


Figure 15: Effect of downward compressive wave over  $L$

Suppose the downward compressive wave reaches to the pile bottom at time  $t_0 + \frac{L}{c}$  travelling full pile length  $L$  (Figure 15). Hence, after  $t_0 + \frac{L}{c}$  time, the relation (Figure 16) between measured force and velocity on pile top element would be.

$$F_3 = Zv_3 \quad 40$$

The Equation 38 represents general downward travelling force at any given time (Salgado 2008).

$$F_d(t) = 1/2(F(t) + Zv(t)) \quad 41$$

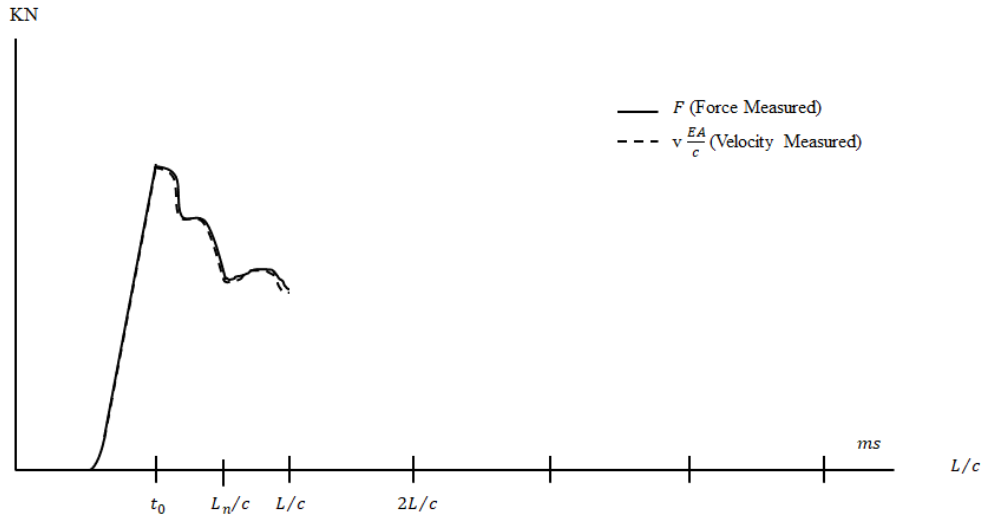


Figure 16: Pile top force and velocity until  $t_0 + \frac{L}{c}$

The downward wave causes pile to penetrate the soil which (penetration) mobilize  $Q_{total}$  amount of soil resistance (Figure 17). This mobilization generates upward compressive wave at time  $t_0 + \frac{L}{c}$  which (wave) is felt by the pile top at  $t_0 + \frac{2L}{c}$ . Therefore the pile top will feel force and velocity due to compressive wave attributed to mobilized soil resistance (Figure 18). Figure 18 indicates only base resistance occurred. If skin resistance also happens, the skin resistance will mobilize the surrounding soil. As a result, an upward compressive wave will be generated which

will divergence of force and velocity curve before  $\frac{2L}{c}$  (Figure 19). At any given time, PDA measures the net experienced force ( $F$ ) velocity ( $v$ ) of piles top due to upward ( $F_u$ ) and downward force ( $F_d$ ). So, the net upward travelling force would be

$$F_u = Q_{total} - F_d \quad 42$$

$$F_{u_{t_0+\frac{2L}{c}}} = Q_{total_{t_0+\frac{2L}{c}}} - F_{d_{t_0}} \quad 43$$

Where,  $F_{u_{t_0+\frac{2L}{c}}}$  is net upward wave force when arrives at pile top,  $Q_{total_{t_0+\frac{2L}{c}}}$  is mobilized soil generated upward wave force when reaches at pile top, and  $F_{d_{t_0}}$  is the downward wave force at piles top at the time of impact. The Equation 44 represents general upward travelling force at any given time in terms of experienced force ( $F$ ) velocity ( $v$ ) of piles top.

$$F_u(t) = 1/2(F(t) - Zv(t)) \quad 44$$

Hence, putting the  $F_u$  and  $F_d$  into Equation 43, the  $Q_{total}$  would be following.

$$Q_{total_{t_0+\frac{2L}{c}}} = \frac{1}{2} [(F + Zv)_{t_0} + (F - Zv)_{t_0+\frac{2L}{c}}] \quad 45$$

It is assumed that  $Q_{total_{t_0+\frac{2L}{c}}}$  is located entirely at the base (Salgado 2008). So, the velocity equation of the piles base is following.

$$v_b = \frac{2}{Z} F_{d_{t_0}} - \frac{1}{Z} Q_{total_{t_0+\frac{2L}{c}}} \quad 46$$

By substituting  $v_b$  into Equation 32 we get

$$Q_{dynamic (base)} = J_c(2F_{d_{t_0}} - Q_{total_{t_0+\frac{2L}{c}}}) \quad 47$$

Following is the derived equation for maximum static resistance.

$$Q_{ult} = Q_{total_{t_0+\frac{2L}{c}}} - J_c(F_{t_0} + Zv_{t_0} - Q_{total_{t_0+\frac{2L}{c}}}) \quad 48$$

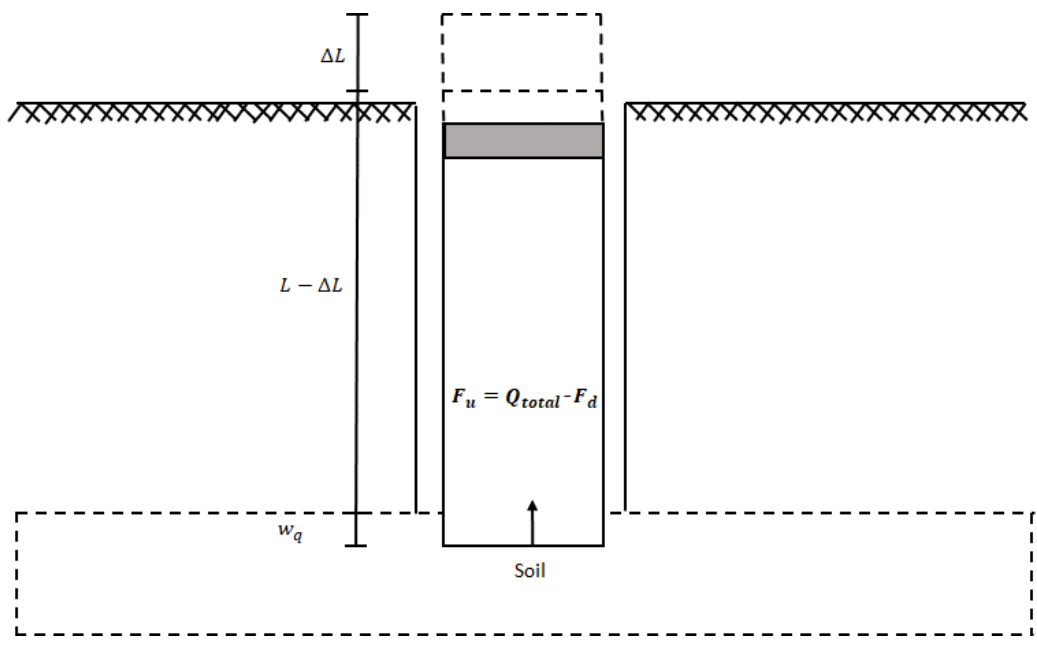


Figure 17: Effect of upward compressive wave over  $L$

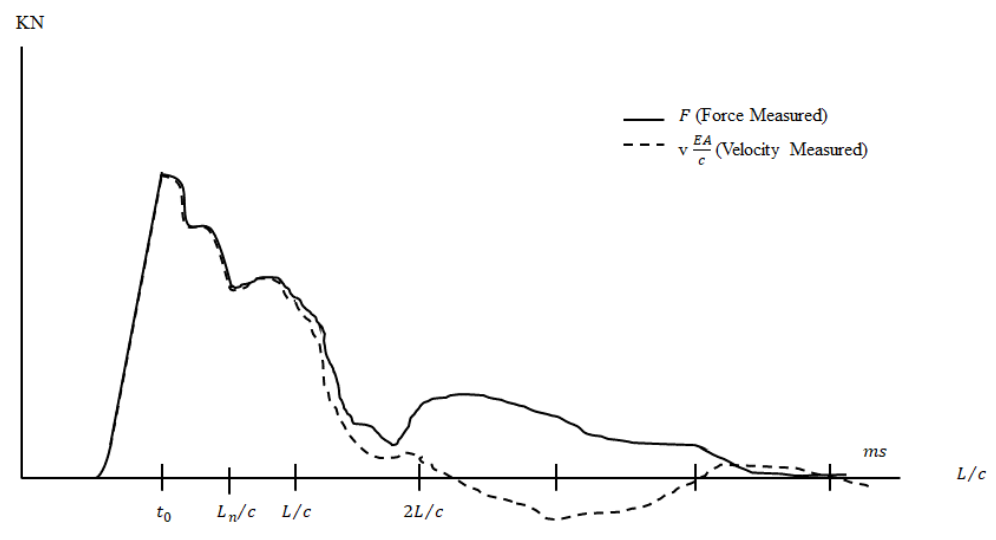


Figure 18: Pile top force and velocity for full time record

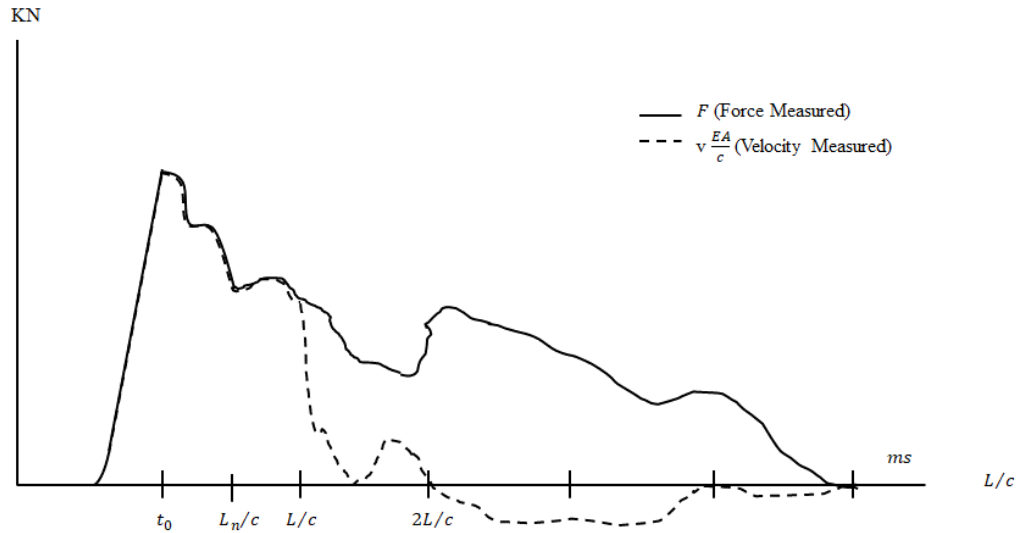


Figure 19: Pile top force and velocity for full time record

### 3.4.2 Bearing Capacity using PDA.

For example, Figure 20 shows a pile top force and velocity for give hammer blow. To calculate the  $Q_{total}$  from the pile top force and velocity,  $F_{t_0}$ ,  $Zv_{t_0}$ ,  $F_{t_0+\frac{2L}{c}}$ ,  $Zv_{t_0+\frac{2L}{c}}$  are needed.

In Figure 20, it can be seen that the value of  $F_{t_0}$ ,  $Zv_{t_0}$ ,  $F_{t_0+\frac{2L}{c}}$ ,  $Zv_{t_0+\frac{2L}{c}}$  are 475 KN, 475 KN, 200

KN and 50 KN respectively. Using Equation 45, the  $Q_{total}$  would be following.

$Q_{total} = \frac{1}{2} * ((475+ 475) + (200-50)) = 550$  KN. Assuming the Case damping factor  $J_c=0.7$ , the

dynamic and static resistance would be following

$Q_{dynamic (base)} = 0.7 * (475 + 475 - 550) = 280$  KN;  $Q_{ult} = 550 - 280 = 270$  KN

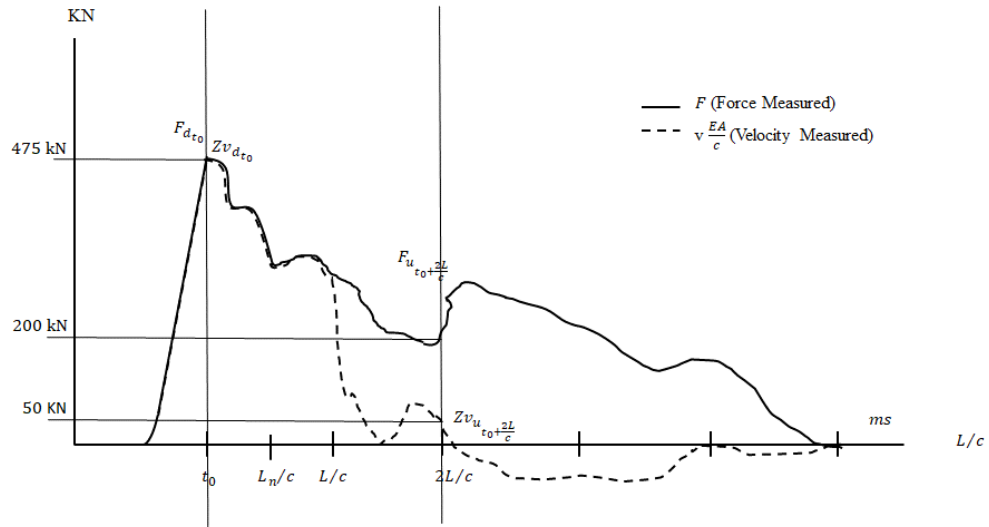


Figure 20: Pile top force and velocity

## CHAPTER 4

### VERIFICATION OF THE PDA ANALYSIS USING FIELD TEST DATA

#### 4.1 Introduction

To verify the PDA data analysis, eight sets of the PDA test results were analyzed. The data sets were collected from two different projects (Banks and Cobb County) in Georgia and one project (Wake County) from North Carolina. From the projects data, values of critical parameters used in PDA were collected. These parameters include blow per inch, rock quality designation (RQD), ground type, maximum hammer energy, pile impedance, required driving resistance, maximum factored structural resistance, applied case damping factor, Case method calculated ultimate pile resistance (static resistance), pile top force and velocity immediately after hammer impact. The pile top force and velocity will immediately be used to calculate the total resistance which includes static and dynamic resistance. With the total resistance, applied damping factor and pile impedance dynamic resistance will be calculated.

The calculated static resistance from all data sets will be compared with dynamic resistance to assess the performance of PDA. The CAPWAP recommended Case damping factor will be given a close look to check how Case damping factor changes against the blow per inch.

#### 4.2 Banks County, Georgia

For PDA result analysis in this research, the seven data sets were collected from a construction (bridge replacement) site in Banks County. Figure 21 shows the layout of the Banks County project where three PDA dynamic tests were executed at Bent 1, Bent 3, and Bent 4. PDA tests of all piles were conducted with a pilot hole. From the three bents a total of seven data sets were shown in this research. In addition, one static load test was executed at Bent 3.

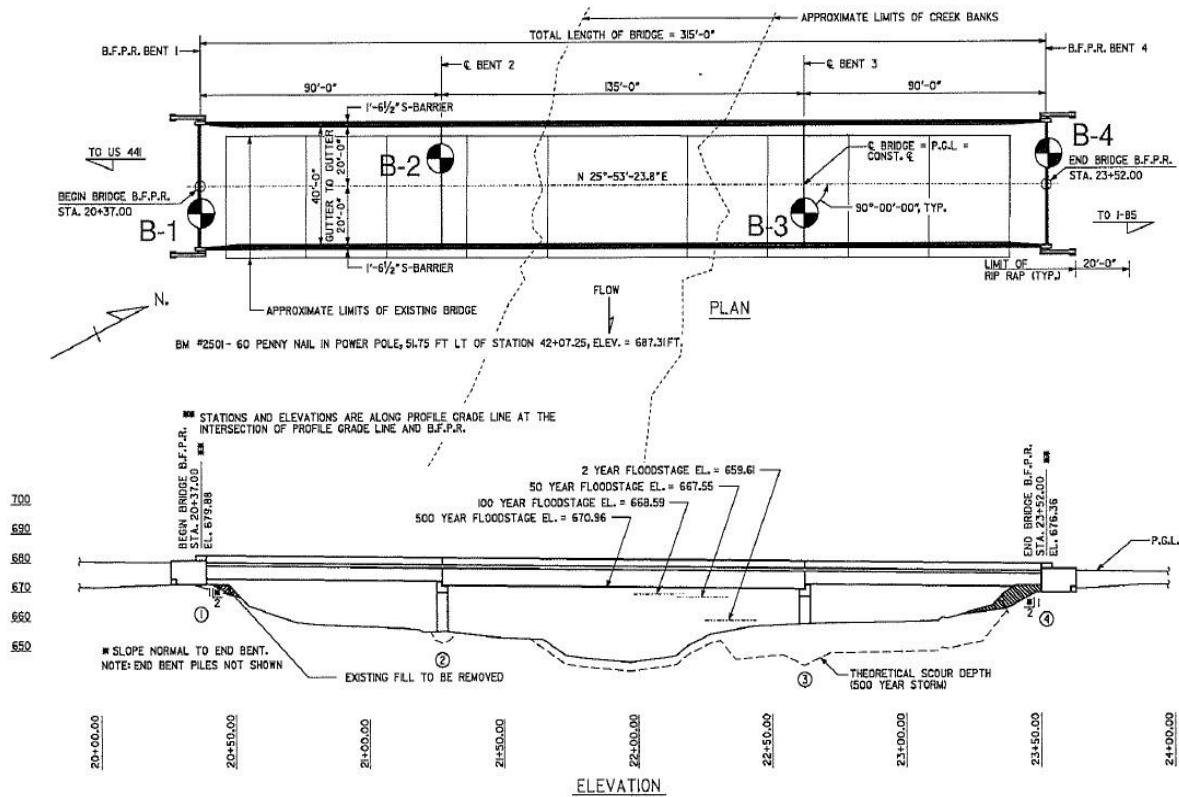


Figure 21: Banks County project layout (GDOT Office of Materials and Testing 2021)

Table 2: Pile design parameters in Banks County

Pile Type	Pile Size (inch)	Nominal Compression and Tension Stress (ksi)	Max Factored Structural Resistance (kips)
HP	14 × 73	45	520
Bents	Maximum Factored Strength Limit State Load (kips)	Maximum Factored Service State Load (kips)	Factored Extreme Event I Limit State Load (kips)
1	319	221	210
3	313	290	223
4	319	221	210

Table 3: Uniaxial compressive strength of the rock samples at bent 3

Bent	Sample	Distance (ft)	Diameter (inch)	Peak Load (lb)	Peak Stress (psi)
3	1	26	1.98	26,458	8,590
	2	28	1.98	44,578	14,480

Table 4: PDA test results in Banks County

Parameter	Bent 1	Bent 3			Bent 4		
Analyzed blow Number	236	4	5	6	95	131	145
Minimum tip elevation (ft)	644	633	633	633	648	648	648
Estimated tip elevation (ft)	623.88	633.31	633.20	633.09	652.1	649.91	652.10
Blow per inch	9	11	11	11	7	7	7
EMX (kip-ft)	20.9	6.1	15.8	16.6	12	13.55	19.70
Required Driving Resistance (kips)	491	482	482	482	491	491	491
Max Factored Structural Resistance (kips)	520	520	520	520	520	520	520
PDA (kips)	600	570	751	801	520	665	858
CAPWAP (kips)	598	534	655	816	463	541	696
Maximum Compression Stress (ksi)	42.4	28.3	39	42.4	25.7	32.2	42.9

CAPWAP: Case Piles Wave Analysis Program

According to the BFI report, hard rock was encountered at elevations of 646 to 626 ft. The geologic formation of the ground is Hornblende Gneiss/Amphibolite formation of the Georgia Piedmont Region.

The parameters used during the pile design process are shown in Table 2. HP 14 × 73 as pile with 45 ksi nominal stress was used for all bents in Banks County. To avoid structural damage of pile, 90 percent of the yield strength of steel was taken as reference line for the stress level during piles driving. The parameters and corresponding values showed in Table 3 were applied pile capacity estimation.

Table 4 shows the summary of PDA results in Banks County. It can be seen that PDA and CAPWAP calculated resistance are more than required driving resistance and maximum factored structural resistance. The maximum stress developed in each pile base are below 90 percent of the yield strength of steel.

### 4.3 Cobb County, Georgia

From Cobb County, two PDA test results from a bridge project, Bob Callan Trail, were used in this research. PDA tests were conducted at Bent 5 and 14 with a pilot hole. Figure 22 shows the layout of the Cobb County project where soil boing B9 is the closest to the Bent 5 location and B7 is the closest to the Bent 5 location.

The test pile encountered the underlying rock immediate after starting of the pile driving. According to the BFI report, the geologic formation of the ground is Factory Shoals Formation and the Chattahoochee Palisades Quartzite Formation. Geology is primarily comprised of biotitic gneiss, mica schist, and amphibolite.

Table 5: Pile design parameters in Cobb County

<b>Pile Type</b>	<b>Pile Size (inch)</b>	<b>Nominal Compression and Tension Stress (ksi)</b>	<b>Max Factored Structural Resistance (kips)</b>
HP	14 × 73	45	520
<b>Bents</b>	<b>Maximum Factored Foundation Load (kips)</b>	<b>Strength Load (kips)</b>	
5	97.84	67.76	
14	97.84	67.76	

The parameters used during the piles design process are shown in Table 5. HP 14 × 73 as piles with 45 ksi nominal stress was used for all bents in Cobb County. To avoid structural damage of pile, 90 percent of the yield strength of steel was taken as reference line for the stress level during piles driving.

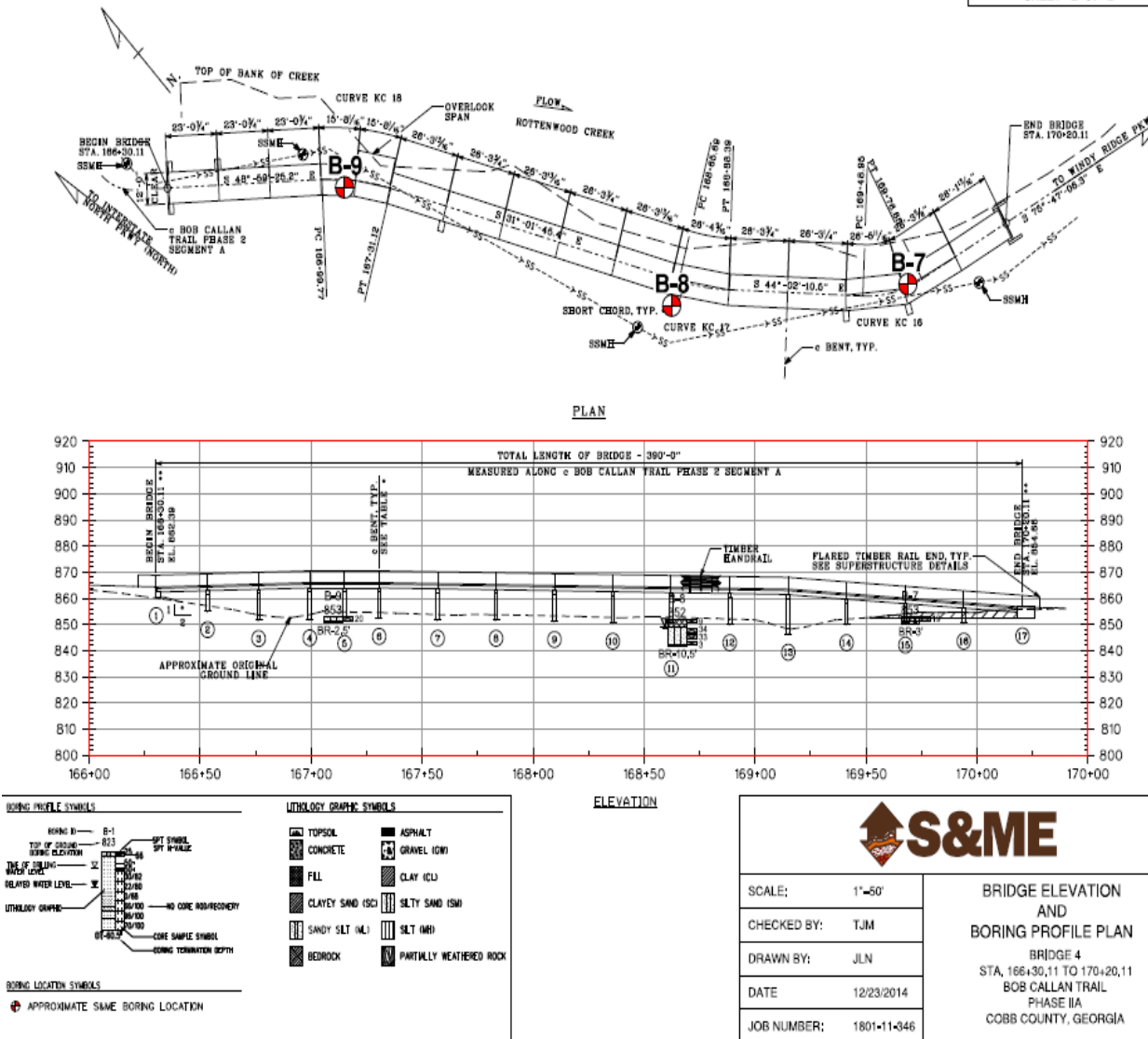


Figure 22: Cobb County project layout of bridge number 4 (GDOT Office of Materials and Testing 2021)

Table 6 shows the summary of PDA results in Cobb County. PDA and CAPWAP calculated resistance are more than required driving resistance. CAPWAP calculated resistance couldn't exceed the maximum factored structural resistance. The maximum stress developed in each pile base is below 90 percent of the yield strength of steel.

Table 6: PDA test results in Cobb County

<b>Parameter</b>	<b>Bent 5</b>	<b>Bent 14</b>
Analyzed blow Number	6	27
Minimum tip elevation (ft)	845	839
Estimated tip elevation (ft)	845	839
Blow per inch	18	20
EMX (kip-ft)	8.6	7.8
Required Driving Resistance (kips)	151	71
Max Factored Structural Resistance (Kips)	520	520
PDA (kips)	766	513
CAPWAP (Kips)	495	417
Maximum Compression Stress (ksi)	40	20.9

#### 4.4 Wake County, North Carolina

For PDA result analysis in this research, one data set was collected from a bridge construction site in Wake County, North Carolina. HP 14 × 73 as pile with 45 ksi nominal stress was used for all bents in Banks County. To avoid structural damage of pile, 90 percent of the yield strength of steel was taken as reference line for the stress level during piles driving.

Table 7: PDA test results in Wake County

<b>Parameter</b>	<b>Bent 1</b>
Analyzed blow Number	5
Minimum tip elevation (ft)	275
Estimated tip elevation (ft)	269.91
Blow per inch	300
EMX (kip-ft)	3.7
Required Driving Resistance (kips)	280
Max Factored Structural Resistance (Kips)	210
PDA (kips)	371
CAPWAP (Kips)	515
Maximum Compression Stress (ksi)	21.3

Table 7 shows the summary of PDA results. PDA and CAPWAP calculated resistance are more than required driving resistance and maximum factored structural resistance. The maximum stress developed in each piles base is below 90 percent of the yield strength of steel.

Table 8: Summary of PDA test input parameters

County	Bent No.	Blow Analyzed	Blow per inch	RQD (%)	Ground type	EMX (k-ft)	Required Driving Resistance (kips)	Applied Case Damping
Banks	1	236	9	100	Gneiss	20.9	491	0.9
	3	4	11	98	Gneiss	6.1	482	0.9
		5		98		15.8	482	0.9
		6		98		16.6	482	0.9
	4	95	7	10	Silty Sand right above	12.0	491	0.9
		131		10		13.55	491	0.9
		145		10	Geiss	19.7	491	0.9
Cobb	14	27	20	N/A	Rock	7.8	71	0.9
	5	6	18	N/A	Rock	8.6	151	0.9
Wake	1	5	300	N/A	Granite	3.7	280	0.43



Figure 23: PDA field test at Banks County, Georgia, USA

Table 7 shows the summary of PDA results. PDA and CAPWAP calculated resistance are more than required driving resistance and maximum factored structural resistance. The maximum stress developed in each piles base is below 90 percent of the yield strength of steel.

Table 8 the preliminary information and input parameters of all PDA test. Same pile impedance (38.2 k-sec/ft) were found in all cases. Silt was encountered for Bent 4, Banks County. For all other tests, rock was encountered. 0.9 case damping factor was used for all tests except in Wake County. The Figure 23 shows the executed PDA test in the Banks County.

## CHAPTER 5

## RESULTS

## 5.1 Analysis of PDA test result

The PDA results are analysed considering the total resistance calculated by PDA. The total driving resistance ( $Q_{\text{total}}$ ) of a pile is comprised of base dynamic resistance ( $Q_{\text{db}}$ ) and maximum static resistance (RMX).

RMX,  $F_{t_0}$ ,  $Zv_{t_0}$ ,  $F_{t_0+\frac{2L}{c}}$ ,  $Zv_{t_0+\frac{2L}{c}}$  and  $J_c$  were collected from the PDA test results from the reviewed projects. The total driving resistance ( $Q_{\text{total}}$ ) was calculated by two different ways to verify the PDA total driving resistance. The total driving resistance ( $Q_{\text{total}}$ ) was first calculated by Equation 45 using  $F_{t_0}$ ,  $Zv_{t_0}$ ,  $F_{t_0+\frac{2L}{c}}$ ,  $Zv_{t_0+\frac{2L}{c}}$  values obtained from the PDA time vs. force-velocity curves. In addition, it is also calculated using Equation 48 with the collected RMX and  $J_c$  from the PDA report and  $F_{t_0}$ , and  $Zv_{t_0}$  from the plots. The selected parameters are provided in Table 9, and each PDA result is also provided in Appendix A.

Using  $F_{t_0}$ ,  $Zv_{t_0}$ ,  $F_{t_0+\frac{2L}{c}}$ ,  $Zv_{t_0+\frac{2L}{c}}$  values obtained from the PDA time vs. force-velocity curves, the total driving resistance ( $Q_{\text{total}}$ ) of each case was calculated. As shown in Table 9, the  $Q_{\text{total}}$  by two different approaches show similar results, which verifies the determination of  $Q_{\text{total}}$  using theoretical equations. The total driving resistance exceeded the required driving resistance in all cases. The total driving resistance ranges from 462 kips at Wake County to 1083 kips at Banks County. The ground conditions of the bearing layers at Wake County and Banks County are granite and gneiss, respectively.

Table 9: Calculated  $Q_{total}$  from two different approaches.

County	Bent No	Blow No.	$F_{t_0}$ (kips)	$Zv_{t_0}$ (kips)	$F_{t_0+\frac{2L}{c}}$ (kips)	$Zv_{t_0+\frac{2L}{c}}$ (kips)	$Q_{total}$ by plot (kips)	RMX (kips)	Case Damping ( $I_c$ )	$Q_{total}$ with RMX (kips)
Banks	1	236	550	575	400	-150	861	600	0.9	850
	3	4	412	412	481	0	690	570	0.9	652.5
		5	580	580	700	0	945	751	0.9	930
		6	610	610	790	0	999	801	0.9	1005
	4	95	525	525	525	-50	771	520	0.9	812.5
		131	550	550	600	0	871	665	0.9	850
		145	666	666	750	-50	1083	858	0.9	1066
Cobb	5	6	450	450	500	-175	829	766	0.9	787.5
	14	27	450	450	375	-75	696	513	0.9	675
Wake	1	5	150	337	375	100	462	371	0.43	475

Based on Equations 48, a general relationship between Case damping factor and RMX can be established that the RMX value decreases as the Case damping factor increases. An example of calculation for Bent 1 at Banks County in Table 10 shows how the damping factor may affect the estimated maximum static resistance. Therefore, damping factors in dynamic analysis of pile needs to be selected carefully.

Table 10: RMX vs Case Damping Factor

Case Damping Factor	0.1	0.5	0.9
RMX (kips)	802	715	600

However, it is common to use a typical value in practice. For example, 0.9 Case damping factor was used in all cases except in Wake County, North Carolina. The maximum pile resistance (RMX) values for all pile exceeded the required driving resistance. Goble et al. (1975) stated that a damping factor is related to the ground condition at the pile tip. When a static load test is conducted along with a PDA, analysis of these two tests provides appropriate damping factor. If a static load test is not available, a damping factor needs to be determined indirectly such as previous experience, published data or simple assumption. Table 1 provided by Ng et al. (2011) is one of

the published information regarding damping factor. However, there is no recommended damping factor for rock in the table probably because a static load test is barely conducted for a pile on rock.

Higher RMX values may not represent the actual maximum pile resistance since the same damping factor used for each test did not appear to be selected for each pile test and its ground condition. This indicates that the PDA results could be questionable. Nevertheless, the PDA has been widely accepted because CAPWAP is known to provide a reasonable estimation of RMX. Consequently, several input parameters including Case damping factors are estimated because of CAPWAP analysis.

Table 11 shows the calculated RMX and Case damping factor by PDA and CAPWAP. The RMX estimated by CAPWAP does not appear to have a clear relationship with the estimated damping factors. Even though the pile capacity (RMX) is generally accepted, it has not been confirmed that CAPWAP Case damping factor represents the true ground conditions especially for rock. Hence, Case damping factor from CAPWAP may need to be verified preferably by static load test. However, it is expected to be very uneconomical.

Table 11: RMX & Case damping factor values from PDA and CAPWAP

County	Bent Number	Blows Number	Blows per Inch	PDA		CAPWAP	
				Damping	RMX (Kips)	Damping	RMX (kips)
Bank	1	236	9	0.9	600	0.4	598
	3	4	11	0.9	570	0.15	554
		5	11	0.9	751	0.46	655
		6	11	0.9	801	0.29	816
	4	95	7	0.9	520	0.13	463
		131	7	0.9	665	0.37	541
		145	7	0.9	858	0.56	696
Cobb	5	6	18	0.9	766	0.76	495
	14	27	20	0.9	513	0.56	417
Wake	1	5	300	0.43	371	0.43	515

Figure 24 demonstrate a relationship between Case damping factor determined by CAPWAP and blow per inch at the end of driving at Banks and Cobb County. Higher blows per inch indicates higher strength of the bearing layer. As damping factor represents ground condition, a solid correlation between the blows per inch and actual damping factor was expected. As shown in Figure 24, the damping factor could be grouped by county showing a good trend in each group. However, it still needs to be interpreted carefully as the other factors affect the penetration of a pile.

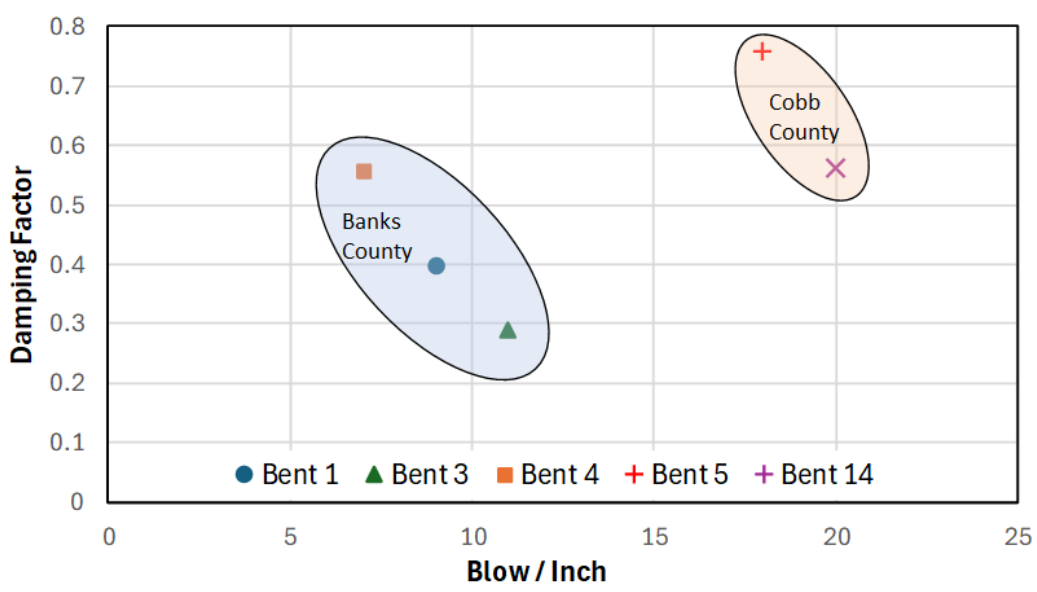


Figure 24: CAPWAP recommended Damping factor vs blows per inch at Banks and Cobb County

## CHAPTER 6

### CONCLUSIONS And RECOMMENDATIONS

The use of pile driving analyser (PDA) for the geotechnical capacity verification of pile has gained popularity due to its simplicity, economic benefits, and proven records of its successful applications. However, the consensus on the application of the PDA on rock has been shared that it may not be appropriate due to the lack of mobilization while driving. Many state agencies have been using alternative options to verify the capacity when installing a pile on rock, which are mostly based on indirect or empirical methods such as bearing refusals or rock properties. On the other hand, it is also known that some practitioners and agencies conduct PDA on pile on rock, as it is believed that the PDA still provides useful information such that the PDA estimated pile capacity is larger than the design capacity and, more practically, pile damage can be monitored during the driving.

This study reviews the theoretical background of the PDA to evaluate the applicability of the PDA on rock. In addition, using actual PDA results, critical parameters are identified by comparing the theoretically calculated and field measured capacity of pile on rocks.

The following conclusions are suggested from the current study.

1. The total driving resistance ( $Q_{total}$ ) calculated by two different approaches shows similar results, which verifies the validity of  $Q_{total}$  by the theoretical equations.
2. Case damping factor in dynamic analysis of pile needs to be selected carefully since it affects the estimation of maximum pile capacity (RMX).
3. It was found that 0.9 of Case damping factor was used in the reviewed projects with PDA. This is believed to be irrelevant to the ground conditions. Therefore, the estimated ultimate

pile capacity (RMX) could be questionable. However, this issue is not supposed to be critical as the final estimation of the pile capacity is estimated by CAPWAP analysis.

4. It has not been confirmed whether the Case damping factor estimated by CAPWAP represents the ground conditions well, especially for rock. Hence, the Case damping factor from CAPWAP still needs to be verified, preferably by static load test. However, it is expected to be very uneconomical for rock; thus, alternative methods are recommended to be investigated.
5. The CAPWAP damping factors grouped by Banks and Cobb Counties show a good trend against blows per inch in each group. However, it still needs to be interpreted carefully as the other factors affect the penetration of a pile.
6. It should be noted that the above analysis was conducted using a limited number of data sets. Nevertheless, this analysis could be a base for future research when more data becomes available.

## REFERENCES

- Abeysinghe, A.B. 2003. "PDA Test as a Method of Pile Testing for Bored and Cast In-Situ Piles End Bearing on Rock." <https://medium.com/@arifwicaksanaa/pengertian-use-case-a7e576e1b6bf>.
- California, and Department of Transportation. 2008. *Foundation Manual*.
- E. A. L. Smith. 1960. "Pile-Driving Analysis by the Wave Equation." *Soil Mechanics and Foundations* 86. <https://doi.org/10.1061/JSFEAQ.0000281>.
- Frank Rausche, Michael Morgano, Pat Hannigan, Marty Bixler, and Jorge Beim. 2006. "Experiences with Heavy Drop Hammer Testing of Rock Socketed Shafts." In *31st ANNUAL CONFERENCE ON DEEP FOUNDATIONS*.
- Goble, G. G., Garland Likins, and Frank Rausche. 1975. "Static Bearing Capacity of Piles From Dynamic Measurements." *Ohio Department of Transportation*, no. March. <https://doi.org/10.1680/iicep.1977.3061>.
- Hiley, A. 1925. "A Formula and Its Application in Piling Practice Explained." *Engineering, London*, no. 6: 657–721.
- Janbu, N. 1953. "An Energy Analysis of Pile Driving Using Non-Dimensional Parameters." *Annales de l'Institut Technique Du Batiment et Des Travaux Publics*, 63–64. <https://www.theworldcounts.com/challenges/planet-earth/state-of-the-planet/world-waste-facts/story>.
- Liu, Chun Lin, Shuo Zhang, Meng Xiong Tang, He Song Hu, Zhen Kun Hou, and Hang Chen. 2020. "Vertical Dynamic Response of Rock-Socketed Piles in a Layered Foundation." *E3S Web of Conferences* 173. <https://doi.org/10.1051/e3sconf/202017304002>.
- Ng, Kam, and Todd Sullivan. 2017. "Case Studies to Demonstrate Challenges of Driven Piles on Rock." *Geotechnical Research* 4 (2): 82–93. <https://doi.org/10.1680/jgere.16.00015>.
- Ng, Kam Weng, Muhannad T. Suleiman, Matthew Roling, Sherif S. AbdelSalam, and Sri Sritharan. 2011. "Development of LRFD Design Procedures for Bridge Piles in Iowa – Field Testing of Steel H-Piles in Clay, Sand, and Mixed Soils and Data Analysis (Volume II)." *IOWA Department of Transportation III* (September): 226. <https://doi.org/10.13140/RG.2.1.3745.3285>.
- Noorzad, Ali, Mehran Karimpour-fard, and Alireza Mohammadi. 2008. "Evaluation of Bearing Capacity of Piles Using the Results of Evaluation of Bearing Capacity of Piles Using the Results of Different Full Scale Pile Load Tests," no. September: 1–6.
- Rausche, Frank, Liqun Liang, Ryan C. Allin, and David Rancman. 2004. "Applications and Correlations of the Wave Equation Analysis Program GRLWEAP." *Proceedings of the Seventh International Conference on the Application of Stresswave Theory to Piles*, no. C: 107–23.
- Salgado, Rodrigo. 2008. *THE ENGINEERING OF FOUNDATIONS*.
- So, Arthur K.O., and Charles W.W. Ng. 2011. "Dynamic Soil Parameters and Case Damping for

High-Capacity Long H-Piles.” *Canadian Geotechnical Journal* 48 (11): 1616–29.  
<https://doi.org/10.1139/t11-064>.

Testing, GDOT Office of Materials and. 2021. *Bridge Foundation Investigation (LRFD) - PI 0015533 Rev.1*.

Wellington, A. M. 1893. “Piles and Pile Driving.” *Engineering News Pub. Co., New York*.

Whitaker, Thomas. 2013. *The Design of Piled Foundations: Structures and Solid Body Mechanics*.

APPENDIX A

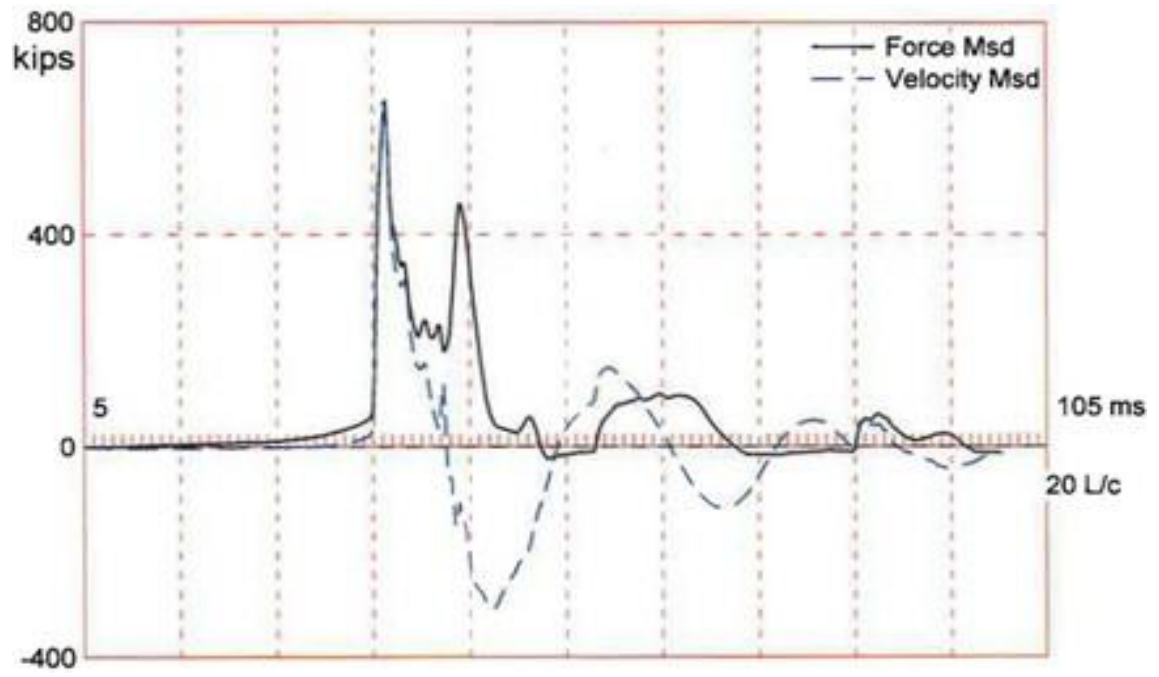


Figure 25: Pile top force and velocity (Bent 1-Blow 236)

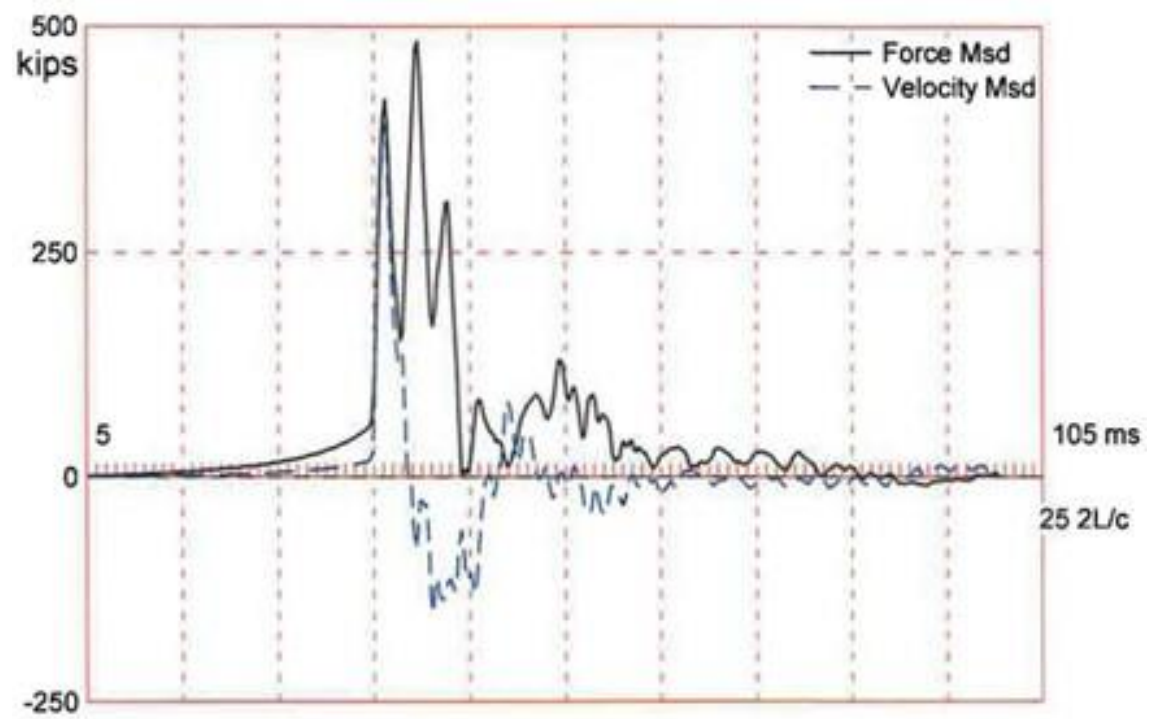


Figure 26: Pile top force and velocity (Bent 3-Blow 4)

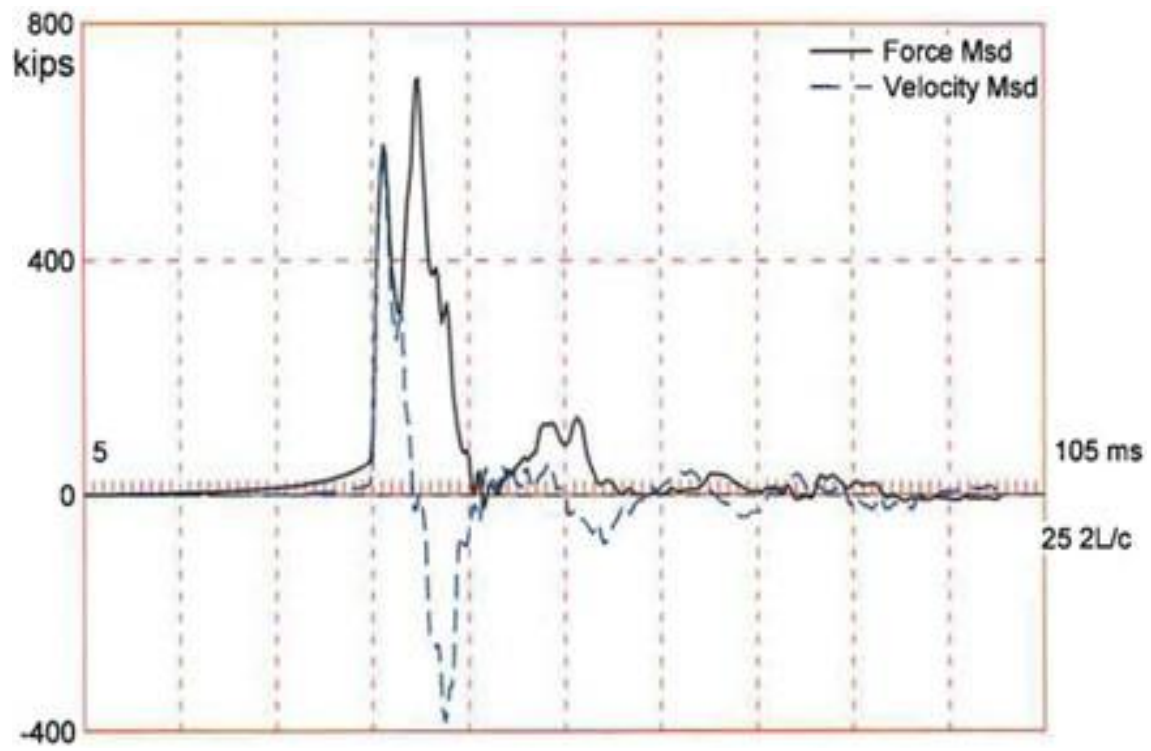


Figure 27: Pile top force and velocity (Bent 3-Blow 5)

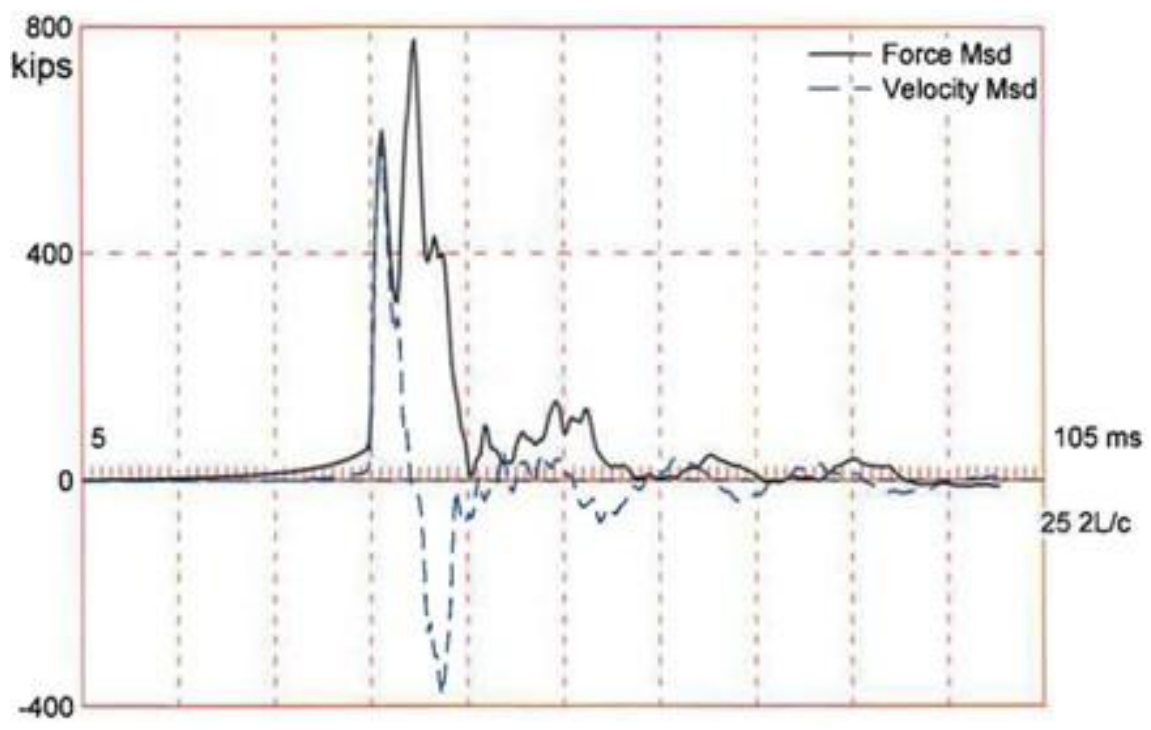


Figure 28: Pile top force and velocity (Bent 3-Blow 6)

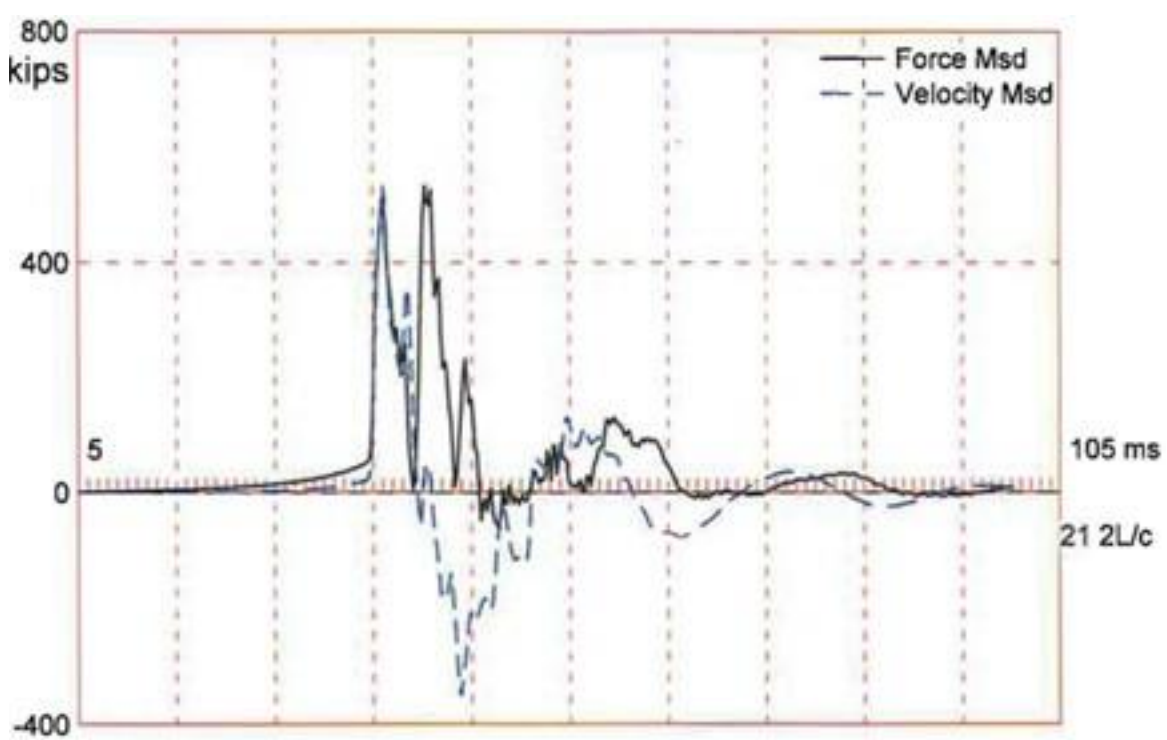


Figure 29: Pile top force and velocity (Bent 4-Blow 95)

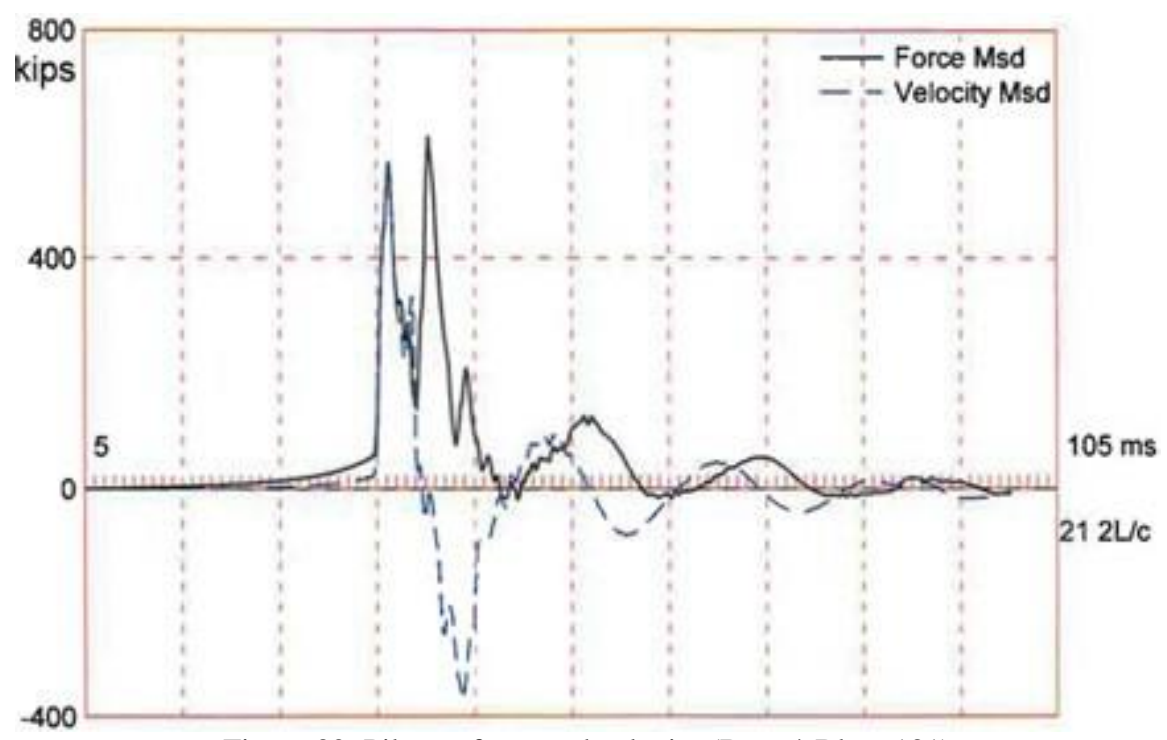


Figure 30: Pile top force and velocity (Bent 4-Blow 131)

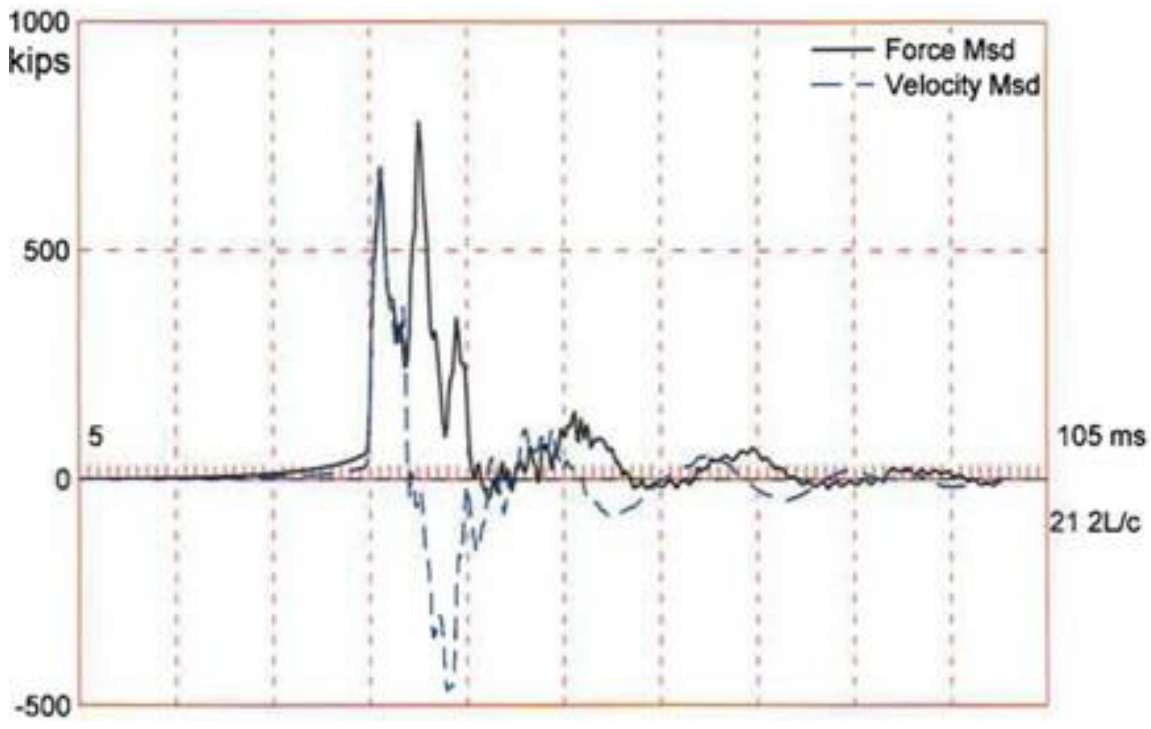


Figure 31: Pile top force and velocity (Bent 4-Blow 145)

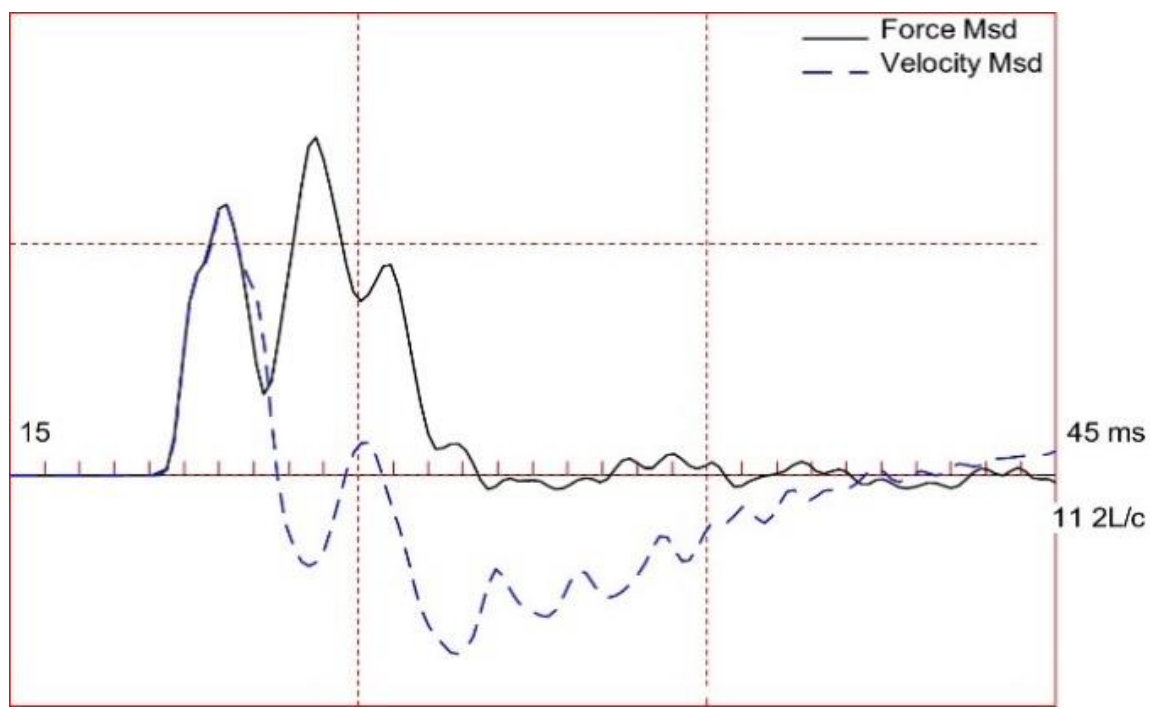


Figure 32: Pile top force and velocity (Bent 5-Blow 6)

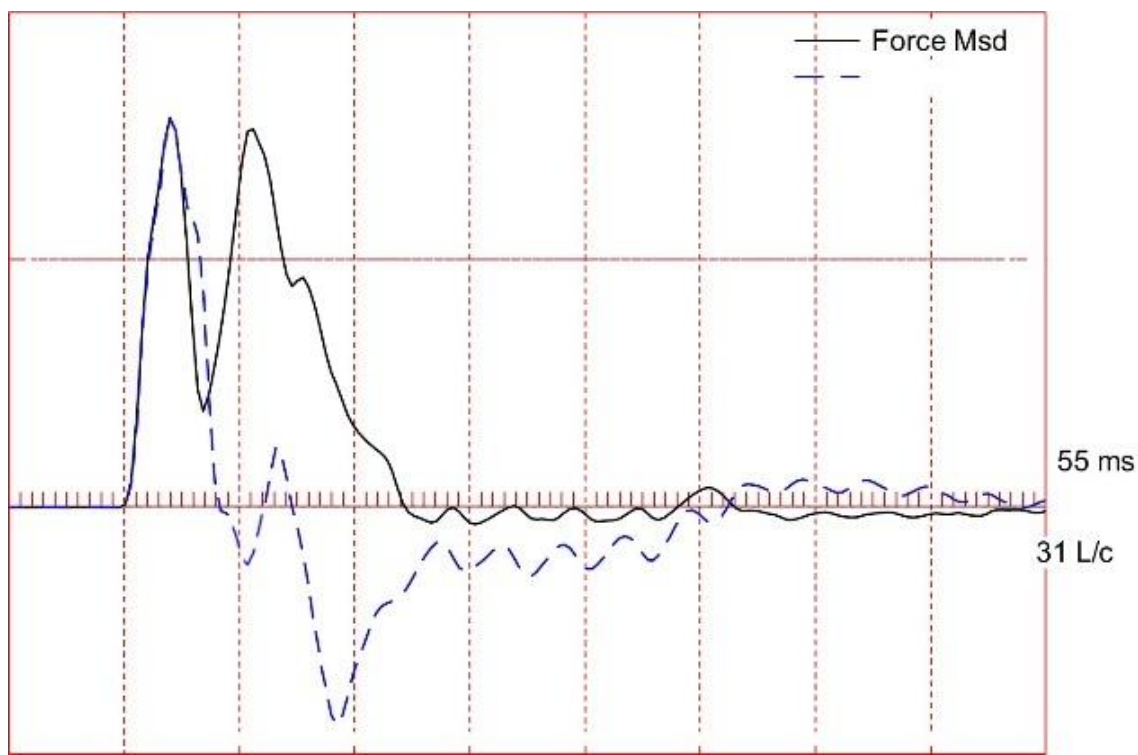


Figure 33: Pile top force and velocity (Bent 14-Blow 27)

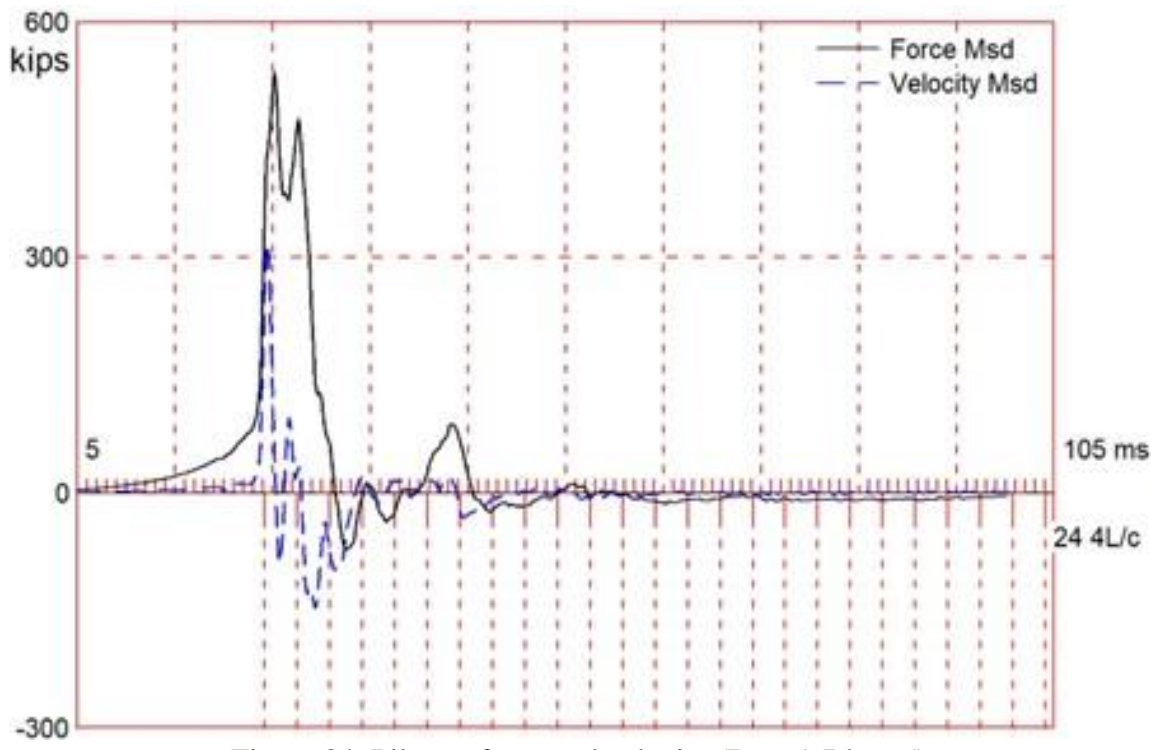


Figure 34: Pile top force and velocity (Bent 1-Blow 5)